Normal and Mutant Rhodopsin Activation Measured with the Early Receptor Current in a Unicellular Expression System

Pragati Shukla* and Jack M. Sullivan*‡

From the *Department of Ophthalmology and ‡Department of Biochemistry, State University of New York, Health Science Center at Syracuse, Syracuse, New York 13210

abstract The early receptor current (ERC) represents molecular charge movement during rhodopsin conformational dynamics. To determine whether this time-resolved assay can probe various aspects of structure–function relationships in rhodopsin, we first measured properties of expressed normal human rhodopsin with ERC recordings. These studies were conducted in single fused giant cells containing on the order of a picogram of regenerated pigment. The action spectrum of the ERC of normal human opsin regenerated with 11-cis-retinal was fit by the human rhodopsin absorbance spectrum. Successive flashes extinguished ERC signals consistent with bleaching of a rhodopsin photopigment with a normal range of photosensitivity. ERC signals followed the univariance principle since millisecond-order relaxation kinetics were independent of the wavelength of the flash stimulus. After signal extinction, dark adaptation without added 11-cis-retinal resulted in spontaneous pigment regeneration from an intracellular store of chromophore remaining from earlier loading. After the ERC was extinguished, 350-nm flashes overlapping metarhodopsin-II absorption promoted immediate recovery of ERC charge motions identified by subsequent 500-nm flashes. Small inverted R_2 signals were seen in response to some 350-nm flashes. These results indicate that the ERC can be photoregenerated from the metarhodopsin-II state. Regeneration with 9-cis-retinal permits recording of ERC signals consistent with flash activation of isorhodopsin. We initiated structure–function studies by measuring ERC signals in cells expressing the D83N and E134Q mutant human rhodopsin pigments. D83N ERCs were simplified in comparison with normal rhodopsin, while E134Q ERCs had only the early phase of charge motion. This study demonstrates that properties of normal rhodopsin can be accurately measured with the ERC assay and that a structure–function investigation of rapid activation processes in analogue and mutant visual pigments is feasible in a live unicellular environment.

key words: photoreceptor • gating currents • conformational activation • phototransduction

INTRODUCTION

Rhodopsin is the visual pigment of the rod photoreceptor and catalyzes the activation of the G-protein, transducin. Seven transmembrane segments of opsin form a pocket to bind 11-cis-retinal (11*c*Ret),[1] forming a chromophore with the lysine (K296) as a protonated Schiff base (PSB^+-H). The chromophore isomerizes to all-trans-retinal within 200 fs (Schoenlein et al., 1991). Energy uptake by the pigment is efficient and related to the steric strain of isomerization and the charge separation of the cationic PSB^+-H from its anionic counterion ($E113^-$) (Birge et al., 1988). Rhodopsin then undergoes a series of thermal transitions over the time scale of picoseconds through milliseconds to achieve the metarhodopsin-II (Meta-II) spectral conformation. At least two critical and sequential proton exchange mechanisms occur during Meta-II formation: the net transfer of the Schiff base proton to the counterion at $E113^-$ and the uptake of two protons into the cytoplasmic membrane surface (Parkes and Liebman, 1984; Arnis et al., 1994; Jager et al., 1994). These charge motions are reflected in transitions between at least two respective Meta-II states (Meta-II_a and Meta-II_b) that share the same absorption (λ_{max} 380 nm). The transition from the Meta-I to the Meta-II state is the only endothermic state change that occurs during the thermal dark reactions. This indicates that the spontaneous transition into these states is associated with a large positive entropy. A significant molecular volume increase occurs during the lifetime of the Meta-II states (Lamola et al., 1974; Arnis and Hofmann, 1993). The causes of volume expansion are likely to involve changes in sidechain interactions within the membrane, movement of α helices, and the configuration of the cytoplasmic loops that are temporally correlated with formation of the R* state, which allows transducin docking (Khorana, 1992; Altenbach et al., 1996; Han et al., 1996). Several critical state transitions in rhodopsin ac-

Address correspondence to Jack M. Sullivan, M.D. Ph.D., Assistant Professor of Ophthalmology and Biochemistry, SUNY Health Science Center, Dept. of Biochemistry Weiskotten Hall, 4255, 750 East Adams St., Syracuse, NY 13210. Fax: 315-464-8750; E-mail: sullivaj@vax.cs.hscsyr.edu

[1]*Abbreviations used in this paper:* 11*c*Ret, 11-cis-retinal; C_{mem}, membrane capacitance; ERC, early receptor current; ERP, early receptor potential; FAF, fatty acid–free; FWHM, full-width-half-maximum; PSB^+-H, protonated Schiff base; P_t, photosensitivity; SNR, signal-to-noise ratio; WT, wild type.

J. Gen. Physiol. © The Rockefeller University Press • 0022-1295/99/11/609/28 $5.00
Volume 114 November 1999 609–636
Released online 11 October 1999
http://www.jgp.org

tivation are thus spectrally silent. Moreover, the underlying molecular biophysics and forces driving these conformational changes remain unsolved. Proton transfer from the Schiff base to $E113^-$ is sufficient to activate a chain of molecular events which result in R* (Longstaff et al., 1986).

Other tools such as Fourier transform infrared spectroscopy or electron spin resonance can sample conformation changes outside the chromophore environment. But, like time-resolved absorption studies, these are currently limited by the need for hundreds of micrograms or milligrams of detergent-extracted and purified rhodopsin, or cysteine mutagenic engineering to allow site-specific attachment of spin probes. Compared with Fourier transform infrared spectroscopy, only the more sensitive electron spin resonance technology can resolve environmental transitions on a millisecond time scale. These tools have nonetheless contributed greatly to our current understanding of the rhodopsin activation process (Farahbakhsh et al., 1993, 1995; Fahmy et al., 1993; Altenbach et al., 1996; Farrens et al., 1996; Kim et al., 1997), but await the development of cellular expression systems where the harvest of milligram-order quantities of mutated visual pigments is less of an experimental limitation (Reeves et al., 1996; Sullivan and Satchwell, 2000).

The early receptor potential (ERP) is a charge redistribution in rhodopsin associated with protein conformational changes (Cone and Pak, 1971). This signal can be measured at the surface of the living eye, across the retina, or across the membrane of single isolated photoreceptor cells. The ERP depends on rhodopsin being uniformly oriented in the plasma membrane and occurs in two distinct phases (Cone and Brown, 1967; Govardovskii, 1979). The depolarizing R_1 component correlates with flash presentation and likely reflects the molecular process of charge separation during isomerization (Trissl, 1982; Birge, 1990a,b), but its underlying mechanism is not yet established. The millisecond-order R_2 phase is hyperpolarizing and correlates with conformational changes leading to the biochemically active R* or Meta-II intermediates (Ebrey, 1968; Hodgkin and O'Bryan, 1977; Spalink and Stieve, 1980; Trissl, 1982). Absorption of light by different "spectral" states of rhodopsin generates unique ERP signals (Cone, 1967; Cone and Cobbs, 1969). This suggests that the "electrical" states of rhodopsin reflect unique charge distributions during conformational changes. Thus, rhodopsin activation results in both spectral and electrical state transitions. A clear correlation has been established between spectral and electrical states (Ebrey, 1968; Cone and Cobbs, 1969; Spalink and Stieve, 1980). However, the measurements of these states reflect different molecular properties. Absorption state transitions reflect the different environments of the chromophore. Since the chromophore lies predominantly in the membrane plane, these transitions reflect principally in-plane charge redistributions. Electrical transitions, which are measured across the membrane, reflect molecular events with vector contributions largely orthogonal to the dipole absorption state of the chromophore environment. Because of this, electrical measurements assess a vector of the activation process that is distinct. An additional advantage is that electrical measurements can simultaneously sample the entire coordinated ensemble of charge motions, dipole reorientations, or interfacial charge transfer reactions across the full thickness of the membrane plane and its local boundary surface layers. With modern cellular electrophysiological tools, charge motions can currently be examined with submillisecond time resolution. Supplementary techniques are likely to extend recording to the nanosecond time domain.

The early receptor current (ERC) of rhodopsin activation is the direct measure of charge flow that underlies the ERP. This nonlinear capacitative current shows saturation, dependent upon the amount of rhodopsin molecules available for activation (Hodgkin and O'Bryan, 1977). Protein conformation-dependent currents are quite common (Honig et al., 1986), probably the best example being the gating currents of ionic channels that have features in common with the ERC such as signal waveform and bandwidth (Bezanilla and Stefani, 1994). Studies of channel gating currents has clarified the role of the molecular structure during voltage-dependent gating. For example, the localization of gating charges to the S4 helices, and the motions of these elements in the electrostatic field, was advanced through gating current studies of expressed ionic channels. Similarly, the ERC might be used to study the forces that govern rhodopsin state transitions while it resides in a physiologically intact membranous environment, or to analyze electrical state transitions that may be spectrally silent to UV-visible or infrared absorption, or occur in environments not accessible to spin probe introduction.

The ERC of rhodopsin activation in intact photoreceptors has been elegantly studied using gigaohm-seal, whole-cell patch clamping techniques (Hestrin and Korenbrot, 1990; Makino et al., 1991). Therefore, techniques were developed in which the ERC could be recorded in a unicellular expression system containing high levels of normal rhodopsin (Sullivan, 1996, 1998; Shukla and Sullivan, 1998; Sullivan and Shukla, 1999; Sullivan et al., 2000). This method allows assay of rhodopsin activation with seven to eight orders of magnitude less material than other time-resolved techniques. High fidelity ERC currents are routinely recorded from single fused giant cells containing on the order of a picogram of regenerated rhodopsin (1.5 $\times$

10^7 molecules). In the current work, the ERC approach is used to investigate activation properties of expressed normal or wild-type (WT) human rhodopsin for comparison to known properties of the native pigment previously studied in situ. Human opsin is expressed and regenerated in a membrane environment of transformed HEK293S kidney cells at densities comparable with that in intact photoreceptors (Sullivan and Shukla, 1999). Properties of the WT human visual pigment studied with the ERC are consistent with charge motions originating from activation of the ground state of rhodopsin, within the normal range of photosensitivity, and according to the principle of univariance. ERC signals can be regenerated not only with 11*c*Ret but also with 9-cis-retinal (9*c*Ret). This is a first step toward analogue pigment investigations with the time-resolved ERC tool. Finally, ERC signals were recorded from two mutant human opsin pigments (D83N, E134Q) that have R_2 relaxation properties distinct from WT. Initial steps are taken toward the development of a quantitative and analytical approach to investigate rhodopsin structure–function relationships using this electrophysiological method. This is especially relevant because the millisecond-order conformational events during rhodopsin activation are now thought to be electrostatically mediated (Fahmy et al., 1995; Shieh et al., 1997). This study is the first to apply the ERC method to characterize rapid electrical processes during activation in expressed mutant and analogue visual pigments in comparison with the normal process. The ERC approach has the sensitivity and temporal resolution to significantly advance knowledge of the underlying molecular biophysical chemistry of rhodopsin activation.

MATERIALS AND METHODS

Cell Culture and Fusion

Human opsin-expressing HEK293S cell lines were used for ERC recordings (Sullivan, 1998). Stable mutant opsin HEK293S cell lines were developed using cytomegalovirus expression vectors that were transfected using calcium phosphate (Chen and Okayama, 1988) and selected in G418 (500 μg/ml). Development and characterization of human opsin cell lines is described elsewhere (Sullivan and Satchwell, 1999). The WT human cell line used in these experiments was WT-12 ($\sim 3 \times 10^6$ opsins/cell), the D83N mutant cell line was D83N-11 ($\sim 8 \times 10^5$ opsins/cell), and the E134Q cell line was E134Q-7 ($\sim 2 \times 10^5$ opsins/cell) (Nathans et al., 1989; Sullivan and Satchwell, 2000). All cell lines were grown at 37°C and 5% CO_2 in DMEM/F12 containing 10% calf serum, antibiotics, and 2.5 mM l-glutamine on poly-l-lysine–coated coverslips. Cells on coverslips were chemically fused to form giant cells by a 1–2 min exposure to 50% (wt/vol) polyethylene glycol (1,500 g/mol) in 75 mM HEPES, pH 8.0 (Boehringer-Mannheim Biochemicals) (Kersting et al., 1989). Giant cells with a single plasma membrane were evident within hours after fusion. ERCs were recorded between 1 and 3 d after fusion. Fused HEK293 cells amplify the amount of expressed integral plasma membrane proteins and allowed high fidelity measurements of sodium channel gating currents (Sheets et al., 1996) and rhodopsin ERCs (Sullivan and Shukla, 1999; Sullivan et al., 2000).

Cellular Pigment Regeneration

Cells on coverslips were washed in regeneration buffer and placed in a light-tight container in the darkroom at room temperature (22–25°C). Regeneration buffer was (mM): 140 NaCl, 5.4 KCl, 1.8 $CaCl_2$, 1.0 $MgCl_2$, 10 glucose, 10 HEPES-NaOH, pH 7.2, and 2% (wt/vol) ($\sim$290 μM) fatty acid–free bovine serum albumin (FAF-BSA; Sigma Chemical Co.). Concentrated (mM) 11*c*Ret or 9*c*Ret stocks (in ethanol) were added in small volumes to this solution to a final concentration of 50 μM in preliminary experiments and 25 μM in the final protocol with 0.025% (vol/vol) α-d-tocopherol (vitamin E) added as an antioxidant. Vitamin E is found in high concentrations in photoreceptor cells and may serve as an antioxidant (Dilley and McConnell, 1970). Vitamin E appeared to improve the longevity and quality of the recordings, likely because of its antioxidation effects on membranes and retinals. Primary regeneration was conducted for at least 30 min and coverslip fragments were then washed in bath recording buffer (without 11*c*Ret or 9*c*Ret) and transferred to the recording chamber, which contained E-1 buffer (see below). FAF-BSA molecules are a pool of chromophore receptors that efficiently solubilize hydrophobic retinals into aqueous solvents and deliver 11*c*Ret loads rapidly and stoichiometrically to regenerate rhodopsin from opsin (Szuts and Harosi, 1991; McDowell, 1993). Optically clear solutions and effective solubilization result when ethanolic stocks of chromophore are introduced into 2% FAF-BSA buffers, whereas without FAF-BSA a scattering dispersion results that is indicative of chromophore partition into aggregates or micelles. Delivery of chromophore to cells is facilitated because a solubilized chromophore can partition more efficaciously into cellular membranes while chromophores bound to FAF-BSA may also be absorbed by pinocytosis. 11*c*Ret was a gift of the National Eye Institute and Dr. Rosalie Crouch (Medical University of South Carolina, Charleston, SC) and 9*c*Ret was obtained from Sigma Chemical Co.

Flash Photolysis

Rhodopsin regenerated in fused giant cells was activated by an intense flash microbeam apparatus described in detail elsewhere (Sullivan, 1998). In brief, light from a xenon flash tube is collimated, filtered, and condensed into a 1-mm-core fused silica fiber optics for transmission to the epifluorescent port of the microscope (Diaphot; Nikon Inc.). The objective lens is used to condense the fiber output into a microbeam spot parafocal with the specimen plane where the giant cell is situated. The spot-size diameter [full-width-half-maximum (FWHM)] in these experiments is 228 μm, which is about three times the size of the largest giant cell used. In routine flash photolysis, three-cavity bandpass filter elements (350, 430, 500, and 570 nm) were used that had 70-nm bandpass (FWHM) centered on peak transmission wavelength. To acquire action spectra data, 30 nm FWHM bandpass filters (centered at 400, 440, 480, 500, 520, 580, and 620 nm, and a 540-nm filter with a 10 nm FWHM bandwidth) were used. The throughputs of all filters, except those at 350 (70) and 400 (30) nm, do not overlap with the absorption spectra of free chromophore (peak $\approx$ 374 nm) such that isomerization (cis $\rightarrow$ trans or trans $\rightarrow$ cis) of any free chromophore is not expected during flashes used to elicit ERCs. Unless otherwise mentioned, flashes were delivered at the maximum capacity of the instrument. Intensities were 10^8–10^9 photons/μm^2 across the near UV/visible band. Flash microbeam intensities were measured using a calibrated photodiode placed over the specimen plane of the microscope. To regulate

flash intensity output (see Fig. 5), the voltage on the flash tube energy storage capacitor was adjusted. Flash duration was only ~14 μs, insuring that the Meta-I ⇔ Meta-II equilibrium (milliseconds) generated at room temperature in these experiments was not perturbed by photoregeneration to other states (Sullivan, 1998). Flash duration did overlap with lifetimes of bathorhodopsin, blue-shifted intermediate, and lumirhodopsin such that photoregeneration from these states is possible. Since we were largely concerned with the millisecond-order R_2 phase of the ERC, any photoregeneration from early bleaching intermediates should not perturb the charge motions occurring during R_2, which correlate with the time scale of the Meta-I ⇔ Meta-II transition. Shielding and fiber optic transmission prevent contamination of the patch-clamp electronics with flash-associated noise.

Photosensitivity (P_t) is the product of quantal efficiency (γ) and the wavelength-dependent absorbance cross section (α_λ). The absorbance cross section of wild-type human rhodopsin is 1.53×10^{-8} μm² (calculated from an extinction coefficient of 40,000 M^{-1} cm^{-1} at 493 nm (Wald and Brown, 1958; Dartnall, 1968; Knowles and Dartnall, 1977) and γ is 0.67, leading to a P_t of 10^{-8} μm² for normal human rhodopsin at peak extinction (493 nm). P_t can be used to estimate the fraction of rhodopsin molecules absorbing at least one photon per flash using the zero-order term of the Poisson equation [$1 - P_o = 1 - \exp(-P_t \cdot i)$], where i is the flash intensity (photons/μm²) and P_o is the fraction that absorbs no photons [Poisson Eq.: $P_n = (P_t{*}i)^n{*}\exp(-P_t{*}i)/n!$, where n is the number of absorptions per chromophore]. In this calculation, one adjusts α_λ by the ratio of absorbance at the wavelength of interest to that at peak extinction. γ is assumed to be constant and independent of wavelength. For the 70-nm bandpass filters used in these experiments (centered at 350, 430, 500, and 570 nm), the fraction of molecules absorbing at least one photon were estimated to be 0.159, 0.716, 0.963, and 0.273, respectively. For the 30- and 10-nm bandpass filters used in these experiments (centered at 400, 440, 480, 500, 520, 540, 580, and 620 nm), the fraction of rhodopsin molecules absorbing at least one photon were estimated at 0.226, 0.626, 0.831, 0.80, 0.733, 0.44, 0.122, and 0.013, respectively. These calculations assume no orientational factors, no self-screening effects, and transparent cellular media. Thus, microbeam flash intensities were not expected to be experimentally limiting for flash photolytic stimulation of expressed rhodopsin pigments, except perhaps for the 620-nm stimulus. The maximum extent of rhodopsin bleaching (i.e., formation of Meta-II) after a single flash is 50% (Williams, 1965, 1974) because of second (or even-numbered) photon reabsorptions during the lifetimes of early states that have high quantal efficiency to photochemically regenerate the ground state (e.g., bathorhodopsin, lumirhodopsin). Flashes at 400, 580, and 620 nm were likely to elicit only single photon absorptions (>90%). Flashes at other wavelengths (440, 480, 500, 520, and 540 nm) were more likely to include even-numbered absorptions (relative fraction of total for even numbered absorptions 0.31, 0.415, 0.405, 0.367, and 0.22, respectively). The absolute flash intensities (10^8 photons/μm²) at the various center wavelengths (parentheses) used in action spectra experiments were as follows: 1.20 (400 nm), 2.29 (440 nm), 2.27 (480 nm), 1.96 (500 nm), 2.02 (520 nm), 1.49 (540 nm), 2.49 (580 nm), and 1.68 (620 nm). The relative ratios of absolute flash intensities relative to that at 500 nm were 0.61, 1.16, 1.15, 1.0, 1.03, 0.76, 1.27, and 0.85, respectively. To scale charge motions for action spectra (see Fig. 3), the reciprocal of these scale factors were used to multiplicatively scale the integrated charge motions.

Whole-Cell ERC Recording

Cells on coverslips were imaged using infrared light (high pass cutoff 830 nm) at 80–160× by an inverted microscope (Diaphot; Nikon Inc.) equipped with Nomarski differential interference contrast, a CCD camera, and a TV monitor. The microscope was housed in a Faraday cage in a dark room. Microelectrodes were fashioned from borosilicate glass using two stage pulls and coated with Black Sylgard (Dow Corning Corp.). Electrodes were routinely filled with one of two intracellular solutions (with or without 10 mM HEPES-CsOH) containing (mM) 70 tetramethylammonium (TMA)-OH, 70 Mes-H, 70 TMA-F, 10 EGTA-CsOH, 10 HEPES-CsOH, pH 6.5; these solutions yielded ERCs with no qualitative changes and are called I-1. The internal pH was chosen to be 6.5 to forward bias the Meta-I ⇔ Meta-II equilibrium strongly in favor of Meta-II (Parkes and Liebman, 1984). In the E134Q experiments, intracellular buffers of otherwise identical composition to I-1 were formulated (I-2, I-3, I-4, I-5) to have intracellular pHs of 6.0, 7.0, 7.5, and 8.0, respectively. Bath solution contained (mM): 140 TMA-OH, 140 Mes-H, 2.0 $CaCl_2$, 2.0 $MgCl_2$, 5.0 HEPES-NaOH, pH 7.0 (E-1). pH was titrated by addition of HCl. Gigaohm seals formed readily with these solutions, electrode/patch/seal capacitance was compensated electronically, and further suction was used to enter whole-cell recording. Inward and outward rectifying conductances are present in HEK293 cells but were suppressed with permeant ion replacement solutions used in the pipette and bath. Without serum used in the growth medium, fused giant cells in E-1 recording buffer rounded up into approximately spherical shapes that remained well attached to the treated coverslips at their base.

The patch-clamp instrument was an Axopatch 1C with a CV-4 resistive feedback headstage and the later was used with a gain of 1 (0.5 Gigaohm feedback resistor; Axon Instruments). Since the ERC is a capacitative current, whole-cell capacitance (C_{mem}) and series resistance were not compensated, because this has the potential to alter the waveform. Membrane holding potential was clamped at 0 mV unless otherwise noted in the legends. Whole-cell capacity current was measured by a +20 mV/4 ms test pulse from a holding potential of −80 mV and C_{mem} was computed by integrating the capacitative current waveform to obtain charge (Q) ($Q/V = C_{mem}$) after substraction of ohmic current. Cell surface area was computed from the measured C_{mem} (1 μF/cm²). Ramp voltage clamps were delivered to test for a high resistance membrane and low level leakage. Cells with large leakage were discarded. Whole-cell currents were recorded at 5 kHz bandwidth using an eight-pole Bessel filter. Flashes were controlled and ERC and flash stimulation data acquired using pCLAMP 5.51 (CLAMPEX) and digitized (200 μs/point) by a Labmaster (100 kHz) interface board (Scientific Solutions Inc.). This acquisition rate was selected to provide the best possible representation of the R_1 signal, which is still undersampled, while critically allowing the full time course of the R_2 component to be acquired out to 100 ms. All ERC data was processed and analyzed using the Origin4.1 package (MicroCal Software, Inc.). Nonlinear least squares fitting was conducted using a Levinberg-Marquardt algorithm.

RESULTS

Giant Cells Generate Large ERCs that Recover Spontaneously with Dark Adaptation

Polyethylene-glycol–fused giant HEK293S cells are used to amplify the amount of regenerable plasma membrane opsin (WT or mutant) in single large cells to improve the signal-to-noise ratio (SNR) during ERC data acquisition. These are prepared from single cells that are stably transformed to constitutively express WT or mutant human opsins in the range of 1–10 × 10^6 molecules (Sullivan and Satchwell, 2000). Giant cells share

with unfused cells a uniform distribution of immunocytochemically reactive opsin in their plasma membranes (not shown). The increased plasma membrane surface area of fused cells contains larger numbers of opsin molecules in linear proportion to the number of cells that participated in the fusion events (Sullivan and Shukla, 1999). R_2 charge motion is linearly dependent on the number of light-activated rhodopsin molecules in the plasma membranes (Cone and Pak, 1971). Therefore, the fused cell system was a rational choice for recording larger ERC signals at greater SNR. The largest fused cells had total WT human ERC R_2 charge (Q) about an order of magnitude greater (2.0 vs. 0.29 pC) than amphibian rod photoreceptors (Makino et al., 1991). Fused cells increased total ERC charge, improved SNR, and allowed spontaneous regeneration of pigment after bleaching by simple dark adaptation without further addition of chromophore beyond the primary regeneration.

Fig. 1 A shows a giant cell ERC obtained on the first flash series (500 nm) after a 30-min regeneration. Flash stimuli were given at 500 nm to extinguish the ERC signal into background whole-cell noise. Both the submillisecond negative R_1 current and the millisecond-order larger, and positive R_2 current were routinely observed and essentially identical to those recorded in photoreceptors (see Hestrin and Korenbrot, 1990; Makino et al., 1991; Sullivan and Shukla, 1999; Sullivan et al., 2000). While not detectable in single unfused cells, in giant cells the R_1 phase of the ERC was recordable, apparently due to increased total rhodopsin and improved SNR. After subtraction of baseline current, integration of each ERC lead to the charge motion (Q_i) in femtocoulombs attributable to each phase. Successive flashes progressively extinguished both phases of the ERC until no responses were observed above background noise. This was consistent with bleaching of plasma membrane rhodopsin due to photolysis. The observation that giant cells spontaneously recovered ERC signals after a complete bleach by simple dark adaptation for 10–15 min without added chromophore was quite surprising. Unless otherwise stated, cells were not exposed to additional 11*c*Ret once the coverslip was removed from regeneration buffer and placed in E-1 buffer in the recording chamber. Subsequent flash photolysis after post-bleach dark adaptation lead to robust ERC signals that were again extinguished by additional flashes at 500 nm (Fig. 1 B). Another period of dark adaptation promoted spontaneous recovery of the ERC that was again extinguished by successive 570-nm flashes (Fig. 1 C). The R_2 but not R_1 signals were recorded after spontaneous regeneration of visual pigment that occurs during 10-min dark adaptation (see discussion).

Fig. 1 D shows the kinetics of the spontaneous recovery of total ERC charge upon dark adaptation for two similarly sized fused cells (67.5 and 65.6 μm diameter). Cells were bleached and dark adaptation was allowed to occur for variable time periods before additional 500-nm flashes were given in rapid succession to extinguish the ERC signal. The total charge (Q_∞) present at each time point of dark adaptation was obtained by summing all Q_i values to yield Q_∞ at that time point. Q_∞ values were normalized to the maximum charge determined for each cell so that regeneration data could be compared. The data were fit by a single exponential accumulation curve. The initial regeneration rate is fast and the process begins to approach steady state by 10 min of dark adaptation. The half time of ERC regeneration was 3.2 ± 1.1 min. If primary regeneration in 2% BSA fully equilibrates WT-HEK293S cells with 11*c*Ret at a concentration (25 μM) in considerable excess over the expected molarity of opsin in fused giant cells (≈2.4 μM), then spontaneous regeneration can be described as a process with pseudo–first order kinetics from a single compartment containing chromophore. We routinely dark adapted cells for either 10 or 15 min between successive extinctions to allow visual pigment and ERC signal recovery to the stationary plateau or, at a minimum, to permit a criterion level of regeneration for any comparison of charge motions under different conditions tested on a single cell.

The Source of Chromophore during Dark Adaptation Is Intracellular

The source of chromophore that promoted spontaneous ERC recovery was investigated. Single fused giant cells regenerated with 11*c*Ret were subjected to primary extinction by successive flashes at 500 nm in normal bath solution (E-1 without chromophore). Dark adaptation promoted spontaneous pigment regeneration and allowed for a secondary extinction of the ERC. Immediately after the second extinction and throughout the next dark adaptation, the chamber volume was replaced with E-1 containing 10 mM hydroxylamine (NH_2OH, pH 7.0) and an additional 5 min of dark adaptation preceded the next series of successive 500-nm flashes. ERCs were elicited and had Q_i values comparable with those seen during the primary and secondary extinctions without NH_2OH. Q_i extinctions before and after NH_2OH are shown (Fig. 2 A). When NH_2OH was present in the bath many more flashes (in this cell 23 flashes) were required to completely extinguish the ERC R_2 charge in comparison to three to five flashes during the primary and secondary extinctions. This suggested that 10 mM NH_2OH decreased photosensitivity and this effect will be examined fully in a subsequent study. Two dark adaptations (10 min each) in 10 mM NH_2OH were followed by some but not full ERC signal recovery, which was then subsequently extinguished by additional flashes.

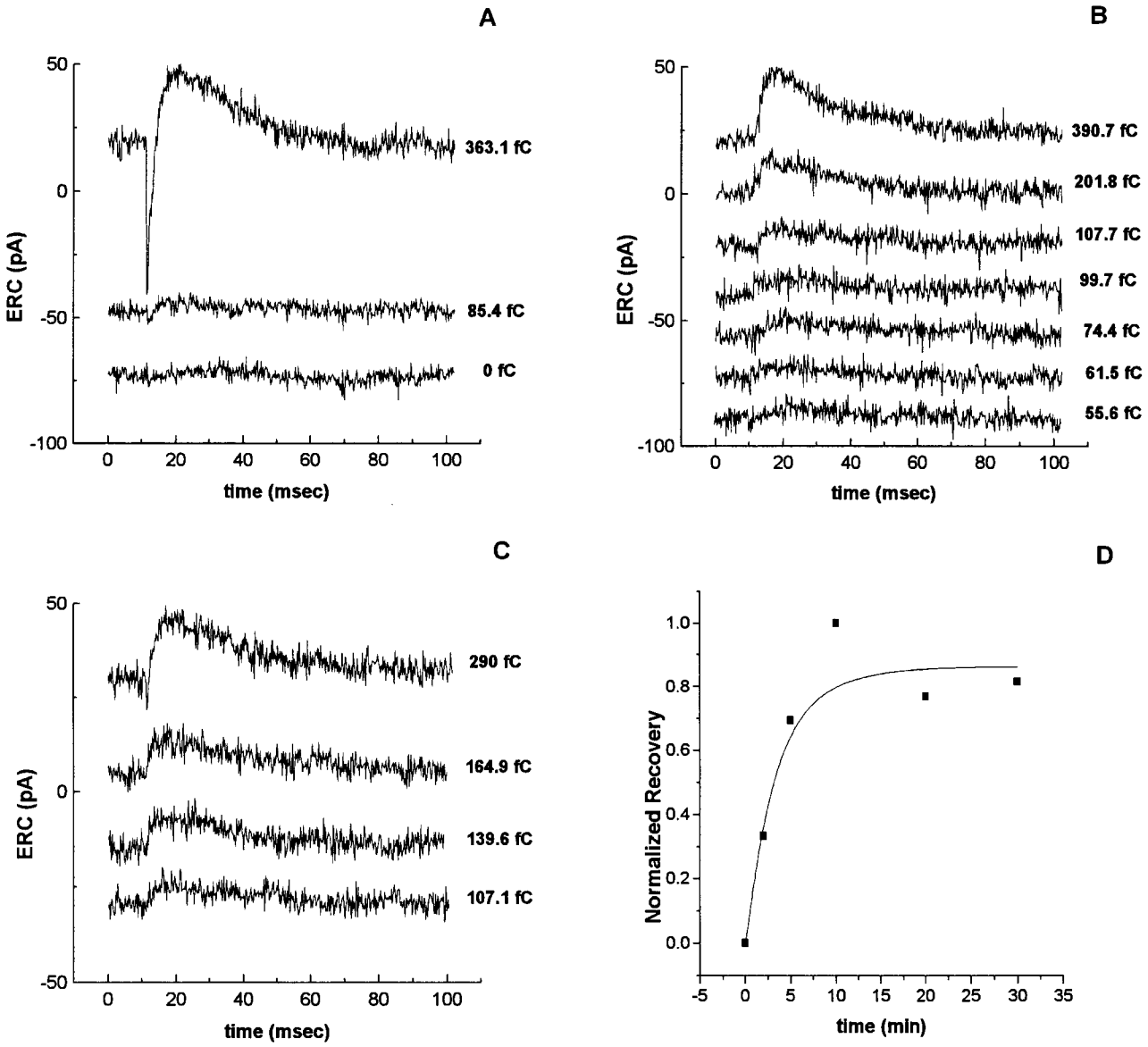

Figure 1. WT ERC currents from fused giant cells. (A) Flashes (500 nm, 4.08×10^8 photons/μm^2) elicited ERC currents that were extinguished by successive stimuli during the first bleach of this cell after primary chromophore regeneration. The integrated R_2 charge motion (Q_i) is shown to the right of each trace. The location of the ERC traces with respect to the ordinate is arbitrary to allow easy comparison. Note the prominent inward R_1 current in the ERC stimulated by the first flash. In this cell, charge was extinguished by the third flash. (B) After a 10-min period of dark adaptation, a second series of 500-nm flashes was given and ERC charge motions had recovered. ERC signals were again extinguished by seven successive flashes. No R_1 signals were elicited in the secondary extinctions. (C) An additional 10-min period of dark adaptation also promoted recovery of the ERC signal, here measured with 570-nm flashes (3.38×10^8 photons/μm^2). (D) Kinetic data shows the normalized amount of ERC charge that recovers over time with dark adaptation following flash extinction (500 nm) of the signal ($n = 2$ cells). An exponential growth function was fit to the data: $Q = a \cdot [1 - \exp(-b \cdot t)]$. From the fit a (0.86256 ± 0.06836 min^{-1}) and b (0.31745 ± 0.10078 min^{-1}) were determined (correlation = 0.96526, $P < 0.001$), where b is the rate of regeneration.

ERC signals continued to be recordable on the time scale of tens of minutes in the presence of constant 10 mM extracellular NH_2OH, a concentration far greater than the initial loading of chromophore (25 μM). Fig. 2 B shows the exhaustion course of Q_i vs. flash number for another giant cell before and after introduction of 10 mM NH_2OH into the bath solution. In NH_2OH total R_2 charge decreased with successive extinctions and dark regenerations until no significant signals remained. Bath solution was then replaced with fresh E-1 containing 25 μM 11*c*Ret in 2% FAF-BSA (without NH_2OH). Strong ERC R_2 signals were regenerated comparable in total charge with that seen during the primary extinction. These experiments demonstrate strong evidence

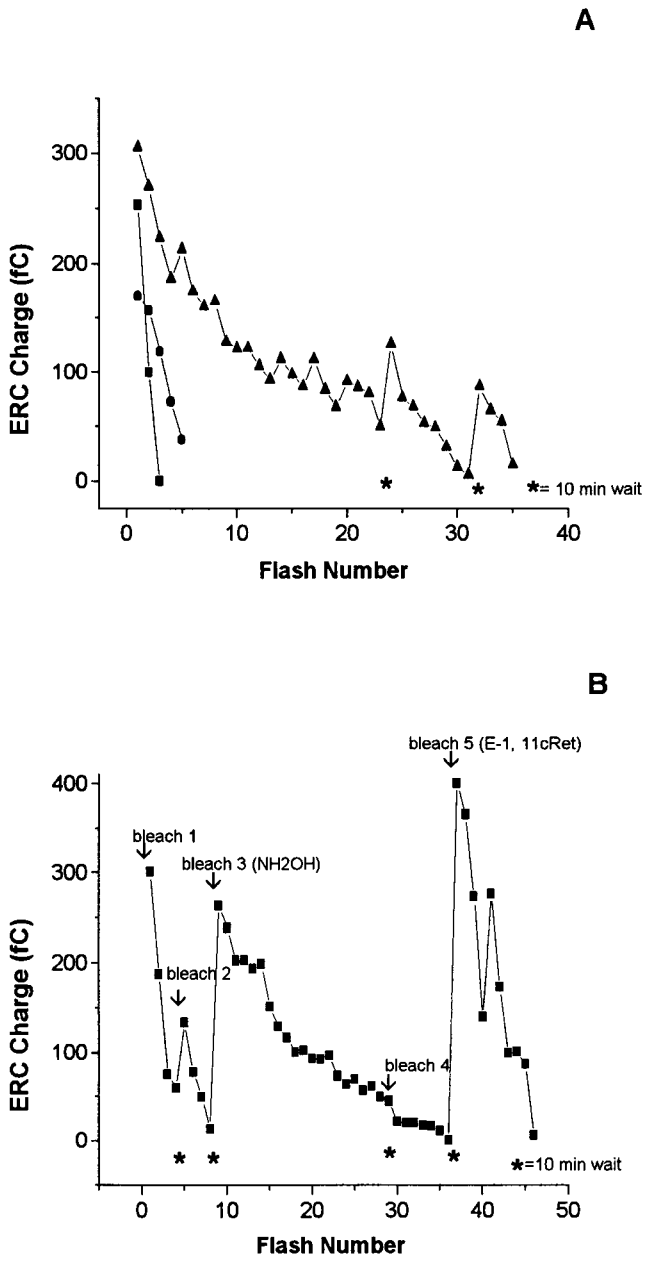

Figure 2. Giant cells spontaneously regenerate from intracellular retinal stores. (A) A giant cell regenerated with 11*c*Ret was subjected to ERC exhaustion with 500-nm flashes (4.08×10^8 photons/μm^2) and the individual R_2 Q_i values were integrated from each ERC and plotted versus flash number. Note the similar photolytic exhaustion of the ERC after primary regeneration (■) and after secondary (spontaneous) recovery (●) during 10 min of dark adaptation. Immediately after the second extinction, 10 mM NH_2OH in E-1 (pH 7.0) was perfused to completely replace the bath solution. This extracellular solution was maintained in the bath for the remainder of the experiment. After 5 additional min, 500-nm flashes were delivered again, but many more flashes were needed to slowly decrement the ERC R_2 charge into extinction (▲). Two 10 min periods of dark adaptation (*) during exposure to NH_2OH permitted some spontaneous regeneration of pigment. (B) A similar but more extensive experiment shows total extinction of the R_2 charge in NH_2OH on the third bleach. Experimental interventions are drawn above the curve. A 10-min dark adaptation showed essentially no pigment regeneration given minimal ERC charge on the fourth extinction. The chamber was then perfused with E-1 to wash out NH_2OH, and then perfused with E-1 containing 25 μM 11*c*Ret in 2% FAF-BSA/0.025% vitamin E. After 10 min of dark adaptation in 11*c*Ret, ERC signals were recovered with a similar level of initial charge (≈400 fC) and similar photosensitivity to bleaching when compared with the first two flash series.

that the source of 11*c*Ret during spontaneous dark regeneration is internal to the cell that is recorded.

Additional observations support an intracellular origin for 11*c*Ret during dark adaptation. First, the cell repeats dark-adaptive ERC regeneration until the signals expire, and then they do not again regenerate unless 11*c*Ret is reapplied to the cell. This rundown is evident in the extinctions in NH_2OH in Fig. 2 and suggests that cells exhaust their store of 11*c*Ret. Second, in some cells the plasma membrane appeared wrinkled or the cytoplasm appeared optically smooth after expiration of ERC signals. This suggested a change in the structure of internal membranes associated with regeneration ability. Finally, the greatest number of "visual cycles" in this study was eight and was encountered in the largest fused giant cells (≈80 μm diameter) and, although not yet systematically investigated, the number of regenerations appeared to scale in proportion to cell size. Given the hydrophobic nature of 11*c*Ret, it is likely that it is stored by partitioning into internal cellular membranes, and then repartitions back to the plasma membrane during dark adaptation to regenerate visual pigment (see discussion).

The ERC Action Spectrum Is Consistent with the WT Human Rhodopsin Photopigment

A previous study of ERC spectral sensitivity used 70-nm bandpass filters and demonstrated a broad action spectrum consistent with the ground state of human rhodopsin pigment (Sullivan and Shukla, 1999). However, the possibility remained that other intermediates such as Meta-III_{465}, pseudophotoproducts ($Meta_{470}$) or even isorhodopsin could contribute to the action spectrum. To investigate this issue further, the spectral sensitivity of ERC R_2 charge motion was measured with stimuli generated with relatively narrow 30-nm bandpass (FWHM) interference filters. In these experiments, the ERC R_2 charge from only the first flash after each 10-min recovery period was obtained between different filter settings. Rather than extinguish the signal, we did a criterion dark adaptation for 10 min between each single flash at a given wavelength. Fig. 3 shows first-flash ERC signals at several different wavelengths from a single giant cell. All ERC signals in the figure were multiplicatively scaled by the ratio of absolute flash intensities measured relative to 500 nm so that the

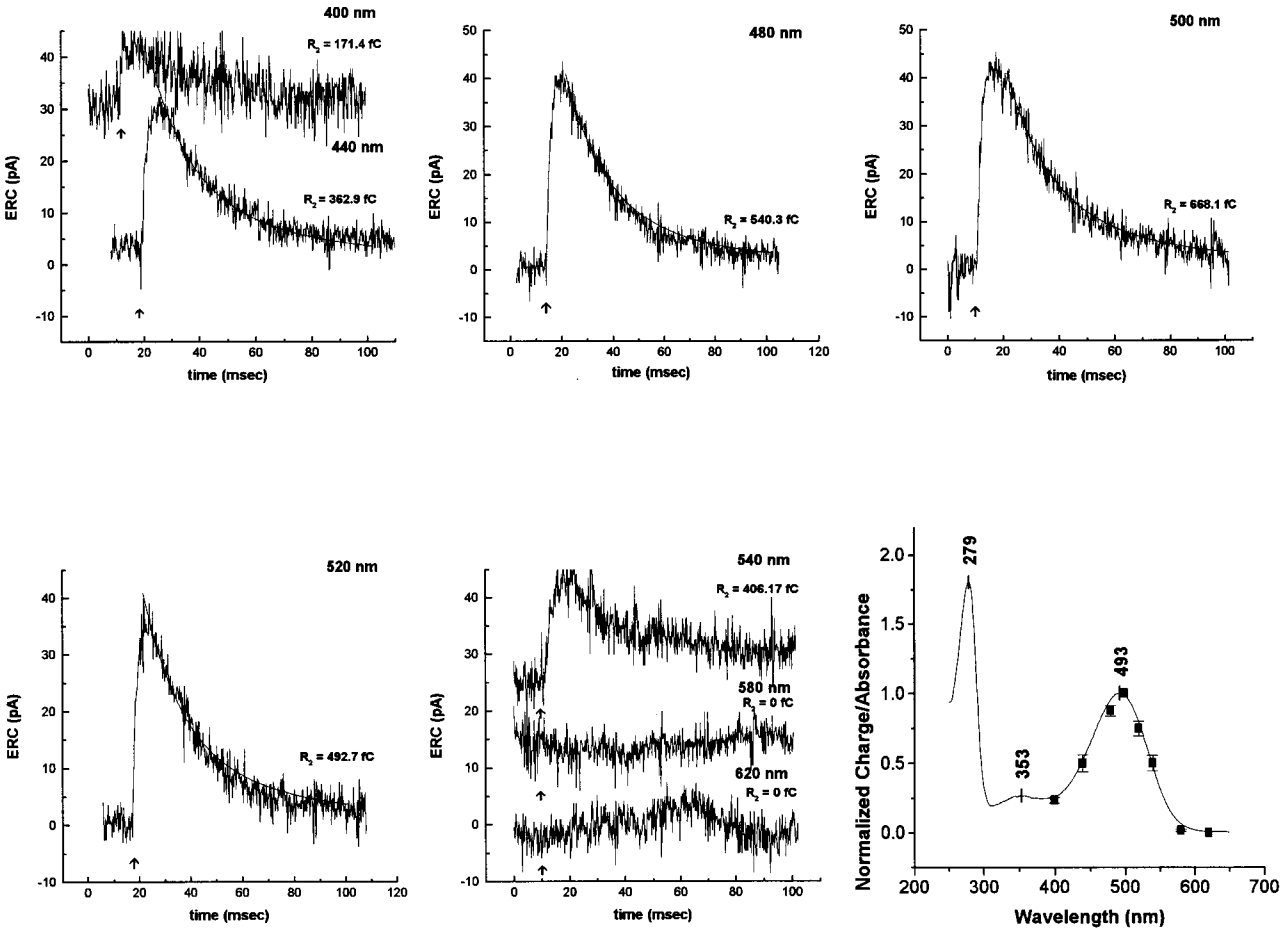

Figure 3. Spectral sensitivity of the ERC response. ERC responses to single initial flashes at several wavelengths are shown. Data was collected from cells after spontaneous dark regenerations. Filters were 30 nm (FWHM) except for the 540-nm filter, which was 10 nm (FWHM) (see materials and methods). For each waveform, the current trace was multiplicatively scaled by the relative ratio of the flash intensities at the test wavelength relative to 500 nm. A double exponential function was fitted to the R_2 relaxation of the 500-nm response. The same function was overlaid with the 440-, 480-, and 520-nm ERC responses and provided a good fit. Action spectra of the R_2 ERC response (bottom right) is shown. For each cell ($n = 3$), a single flash was given at each wavelength with a 10-min period of dark adaptation between each flash. Single flashes were given so that cells would be less exhausted and regeneration would be more uniform over recording epochs at different wavelengths. The integrated R_2 charge, Q_i, was obtained at each wavelength. Q_i values for each cell were multiplicatively scaled by the ratio of photon densities (relative to 500 nm) so that the ERC responses at equal numbers of photons were obtained at the respective wavelengths. R_2 charges were normalized to the maximum charge for a cell to compensate for differences in fused cell rhodopsin content and allow statistical comparison of action spectra. The means (±SEM) are plotted versus wavelength. The variance about the mean at 500 nm is artifactually low because of the normalization procedure. In one cell, holding potential was +30 mV, while in the other two it was 0 mV. Spectra were not affected by this change in holding potential. The absorbance spectrum of human rhodopsin regenerated with 11*c*Ret and purified from WT-HEK293 cells was normalized to the α band peak extinction at 493 nm and plotted over the normalized mean ERC action spectrum on the same abscissa.

spectral sensitivity can be more readily appreciated by observation. The ERC currents vary in amplitude depending on the wavelength of stimulation. To generate the action spectrum, the ERC charge (Q_i) was obtained at each wavelength and the charges were corrected for differences in photon density delivered with different filters so that action spectra at equal photon exposure would be generated. To allow comparison of action spectra from different fused cells containing different amounts of rhodopsin and ERC signal size, spectral sensitivity data were normalized to the maximum integrated R_2 charge at whatever wavelength it occurred. For all three cells, the largest R_2 charge occurred with 500-nm stimulation. In Fig. 3, the mean ERC spectral sensitivity data (±SEM, $n = 3$) are plotted versus wavelength of peak stimulation. By stimulating with only a single flash at each wavelength and allowing sufficient time for regeneration, less stress is placed on the retinal load in the cell and the relative percent of bleaching is considerably less than when the ERC was extinguished by successive flashes at a single wavelength. This should allow greater sensitivity to detect differ-

ences because the fraction of pigment that must regenerate between each single flash bleach is smaller and data can be obtained from a uniformly regenerated population of pigment molecules with low variability.

Instead of fitting spectral sensitivity data with a Lorenztian/Gaussian peak function (e.g., Voigt) (Sullivan and Shukla, 1999), the absorbance spectrum of WT human rhodopsin was normalized with respect to the maximum visible band at 493 nm (α band) and overlaid with the ERC action spectrum. WT rhodopsin was immunoaffinity purified from the same WT-expressing cell line used in these ERC experiments (Sullivan and Satchwell, 2000). The absorbance spectrum of WT human rhodopsin (α band peak at 493 nm) provides an excellent fit to the ERC action spectrum obtained from cells expressing WT human opsin that was regenerated with 11*c*Ret. The ERC action spectrum peaked around 493 nm, consistent with the major absorption band of ground state human rhodopsin regenerated with 11*c*Ret. Moreover, the bandwidth of the α peak of the human rhodopsin absorbance spectrum also fits the ERC data well. It is important to mention that all of the action spectra data were obtained from cells after they had undergone a primary bleach; that is, under conditions where long-lived bleaching intermediates or photoregenerated pigments might have been present. Normal human rhodopsin has an absorbance spectrum that is slightly blue shifted (≈493 nm) with respect to the bovine pigment (498 nm) (Wald and Brown, 1958), and this is maintained on expressing human rhodopsin in HEK293S cells. Assuming that absorption maxima of spectral states of human rhodopsin would scale relative to the bovine pigment (isorhodopsin$_{487}$, Meta-III$_{465}$, and Meta$_{470}$), one would expect peaks at 482, 460, and 465 nm, respectively, in the human pigment. Therefore, if there are spectral states of bleaching intermediates or isorhodopsin present during ERC data acquisition, then they must represent a very small unresolved component of the charge motion. From this we conclude that the pigment underlying the expression ERC is WT human rhodopsin, and that during dark adaptation 11*c*Ret from within the cell reacts with bleached opsin to form a PSB^+-H and a normal ground state pigment.

ERC Extinction Measures Bleaching of Rod Rhodopsin

Successive flashes at a single wavelength and intensity promoted progressive loss of ERC R_2 charge until no further signal was obtained above background current noise. Since the interstimulus intervals between successive flashes were only ∼10 s, pigment regeneration was minimal between stimuli, and regeneration should not contribute to the extinction progression. The spectral sensitivity of the ERC governs not only the efficacy of successive bleaches, but also single bleaches. Fig. 4 A shows the Q_i extinction of R_2 in response to successive flashes at 570 and then 500 nm in a single giant cell. Cumulative flash intensity delivered is used as the dependent variable. After ERC charge was effectively extinguished into noise by 570-nm flashes, 500-nm flashes of greater effective intensity were immediately delivered. The additional extinguishable ERC charge found with 500-nm flashes indicated residual ground state rhodopsin in the cell after the 570-nm flashes. This resulted because 570-nm flashes are not as effective at eliciting ERC currents as are flashes at 500 nm given the relative absorbance of WT human rhodopsin at 570 vs. 493 nm (peak absorbance) (OD_{570}/OD_{493} = 0.436) (Wald and Brown, 1958). Similar findings occur when bleaching at other wavelengths is followed by flash photolysis at 500 nm. The relative probability of activating rhodopsin, taken as the ratio of absorbance cross sections, is only ∼12% at 570 nm relative to 500 nm ($\alpha_{570}/\alpha_{493}$ = 0.115), assuming equal photon density at the two wavelengths. At the maximal flash strengths used, the fraction of rhodopsin molecules absorbing at least one photon at 500 vs. 570 nm was estimated to be ∼0.96 and 0.27, respectively. Thus, the flash system does not deliver sufficient photons at 570 nm to compensate for the lower probability of activation. This illustrates that detection of rhodopsin charge motions depends on the unitary charge motion, which should be the same at any wavelength (see univariance below), and the number of activated rhodopsin molecules that mobilize charge and sum into an ensemble ERC current. Even at peak wavelength (≈500 nm), a given flash intensity may not be sufficient to generate ERC currents above noise because the ensemble ERC current lies within the noise band.

Single exponential exhaustion curves are fit for both data sets at the two respective wavelengths. ERC extinction data for 570-, 500-, or 430-nm flashes from many experiments were always fit by single exponential curves. This is consistent with the ERC charge motion being proportional to the amount of rhodopsin that remains unactivated before each flash is given. Extinction data were fit by the following model using a nonlinear least squares method:

$$Q_i = Q_\infty \cdot \exp(-I \cdot P_t), \quad (1)$$

where Q_i is the charge motion resulting from a single flash, Q_∞ is the total charge before any flashes are given, I is the cumulative flash intensity, and P_t is the photosensitivity. The bleaching process follows an exponential extinction that was further tested by a natural logarithmic transform of Q_i values and linear fitting (Fig. 4 B). Eq. 1 was used to determine P_t for several giant cells subjected to flash photolytic exhaustion under conditions of different flash stimulation wavelength. The charge extinction data for the initial (primary) and

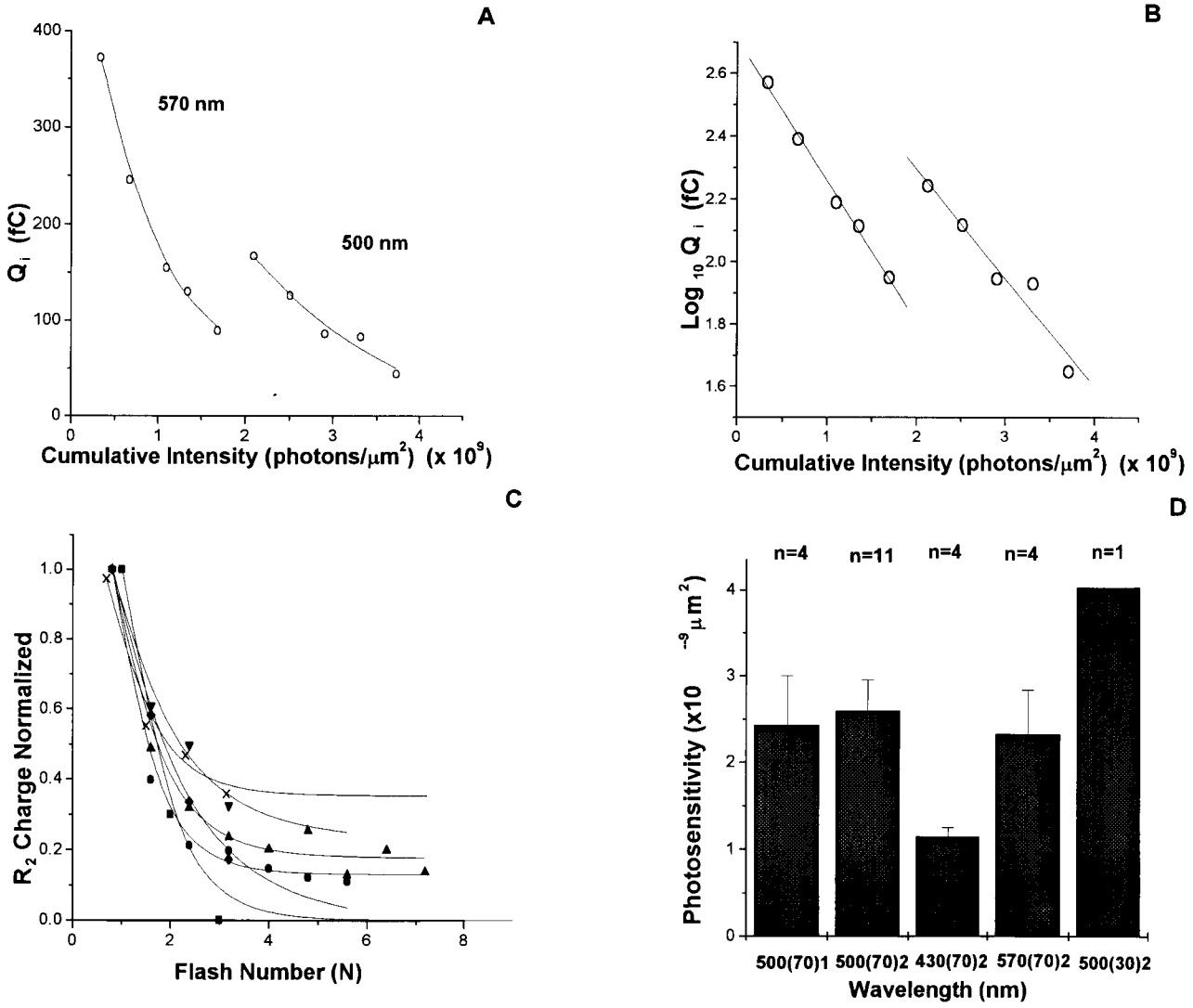

Figure 4. ERC exhaustion photosensitivity is consistent with rhodopsin bleaching. ERC currents (not shown) from a giant cell were recorded in response to flashes at 570 nm (70). Once the 570-nm flashes no longer generated ERC signals above noise, more effective 500-nm flashes were given that activated the remaining unbleached rhodopsin in the cell. The cell was held at +30 mV. R_2 charges were obtained by integrating each ERC signal and plotted versus cumulative photon density for a single bleach. 570-nm flashes promoted progressive loss of ERC charge and 500-nm flashes were able to promote further extinction of ERC charge after the 570-nm flashes were no longer effective. Exhaustion curves at the two wavelengths were fit independently to Eq. 1. (B) The logarithmic transform of the Q_i values was plotted on a linear cumulative intensity scale and lines were fit to both 570- and 500-nm components of the overall R_2 charge extinction. (C) A collage of ERC exhaustion trials for a single large giant cell held at 0 mV is shown. The primary extinction (■) and three later secondary extinctions at 500 nm (●, ▲, and ▼) are shown as well as single extinctions at 570 (×) and 430 (◆) nm. In all cases, the flashes promoted a progressive decrease in ERC charge with successive flash number at constant stimulus intensity (500 nm: 4.08×10^8, 430 nm: 3.62×10^8, and 570 nm: 3.38×10^8 photons/μm^2). The three extinctions at 500 nm resulted in similar exhaustion curves and P_t estimates. (D) By fitting a single exponential decay model (Eq. 1) to data from many experiments ($n = 7$ cells, 24 extinctions), P_t was determined. The means (±SEM) of P_t are plotted for primary bleaches (1), secondary bleaches (2), and at different wavelengths generated by 70-nm bandwidth filters [500(70), 430(70), and 570(70)] or 30-nm bandwidth filters [500(30)]. Data were collected from five cells held at 0-mV holding potential and two cells held at +30 mV. Means for P_t were not different on the basis of parametric (one-way analysis of variance) and nonparametric (Kruskal-Wallis analysis of variance) tests.

three subsequent (secondary) bleaches at 500 nm and single bleaches at 430 and 570 nm in a single large giant cell (≈80 μm) are shown in Fig. 4 C. The charge extinction data sets for each bleach were normalized to the maximum charge on the first flash, and then Eq. 1 was fit to each data set and overlaid. The fit by the single exponential model implies that each flash promoted activation and extinction (bleaching) of a fraction of remaining ground state pigment. In some flash stimulation series, there was a residual content of charge that was slow to extinguish (10–20%). P_t for the primary bleach at 500 nm was estimated to be ~3.3 ×

10^{-9} μm^2, but this is less reliable as there were only three points to fit. The P_t values obtained from fitted curves at 500 nm for the three secondary bleaches were 3.28×10^{-9}, 3.04×10^{-9}, and 2.24×10^{-9} μm^2. P_t was stable over successive secondary bleaches and similar to that of the primary bleach. This is evidence in addition to the action spectrum that the ground state of rhodopsin is regenerated with 11*c*Ret during dark adaptation between successive flash cycles and there was no accumulation of other intermediates with significantly different photosensitivities. The mean ($\pm$SEM) for P_t values from several cells are shown in Fig. 4 D at 500(70), 430(70), 570(70), and 500(30) nm, where the filter bandwidth is indicated parenthetically. Both parametric and nonparametric (Kruskal-Wallis) analysis of variance tests were used to evaluate whether the means of the five conditions were different. No statistically significant difference was found between P_t estimates of human rhodopsin during the initial and secondary extinctions after spontaneous regeneration. However, the trend toward a lower P_t at 430 nm is consistent with the ratio of absorbance of rhodopsin at 430 vs. 500 nm ($\alpha_{430}/\alpha_{493} = 0.423$) (Schneider et al., 1939).

The P_t of WT human rhodopsin is estimated to be $\sim 1.0 \times 10^{-8}$ μm^2 (see materials and methods). The mean value of P_t [500(70) nm] determined from 11 extinctions in 6 cells, all after spontaneous regeneration was $2.6 \pm 0.4 \times 10^{-9}$ μm^2 and the maximum value measured was $5.0 \times 10^{-9} \mu m^2$. P_t values measured using the extinction of R_2 charge are consistent with but lower than that expected of a rhodopsin chromophore. This is likely due to the suppressive effect on P_t of photoregeneration resulting from multiple photon absorptions per rhodopsin molecule at the flash intensities used. For example, with each 500(70)-nm flash, the estimates on even numbered absorptions are $\sim$50%, which would underestimate P_t by a similar amount (see discussion). In recent experiments, stimulus intensity (at 500 nm) was reduced (by 85%) to decrease the probability of multiple hits per molecule, allowing P_t estimation to a mean value of 8.5×10^{-9} μm^2, which approximates that expected from the extinction coefficient (Brueggemann and Sullivan, manuscript in preparation).

Tests of Linearity and the Univariance Principle with ERC Measurements

As first demonstrated by Makino et al. (1991), the ERC of photoreceptors has invariant kinetics regardless of the wavelength or intensity of the flash, although the amplitude of the signal scales in linear proportion to the amount of rhodopsin activated, provided that the flash strength is below saturation. Any rhodopsin molecule absorbing a single or odd number of photons will have a finite probability (constant $\gamma = 0.67$) of successful activation and will contribute to the kinetics of ERC charge flow. At fixed wavelength, variation in stimulus intensity is expected to affect the probability of absorption if each activated rhodopsin molecule makes an independent and additive (linear) contribution to the ERC, and photoreversal to other states by second photon absorptions is minimal. Fig. 5 shows ERCs resulting from 500-nm stimulation at two different flash strengths. When these responses are normalized and overlaid for comparison, the kinetics of the R_2 relaxation at different intensities are not distinguishable. The ERC response versus flash intensity was measured. The Q_i response of the first flash in an extinction series at a constant intensity is plotted versus intensity. A linear fit of the charge motion versus absolute intensity was found. This indicated that the flash intensities used were below saturation for the cellular expression system. This result is consistent with known properties of the ERC/ERP. Each activated rhodopsin molecule undergoes conformational changes to contribute a quantum of charge motion to the overall R_2 signal (Cone and Pak, 1971; Hodgkin and O'Bryan, 1977).

According to the univariance principle, the energy of the photon (wavelength) should not affect the activation kinetics of independent rhodopsin molecules. Photon energy only affects the probability of absorption because the molecular cross section is a function of wavelength. Fig. 6 shows ERCs acquired from a giant cell at 430, 500, and 570 nm. ERC waveforms were normalized to the smoothed peak of the R_2 current for comparison. A double exponential curve was generated to fit the relaxation kinetics of the R_2 signal from the 500-nm stimulus. This template was then overlaid with the R_2 signals from the 430- and 570-nm responses. The 500-nm template fits the R_2 relaxations of the 430- and 570-nm responses rather well, even though the SNR was lower with 570-nm stimuli because the absolute response was smaller. Although the amplitudes of the ERCs and total charge motion of the R_2 signal vary with wavelength, the kinetics of R_2 relaxation are similar. Similarly, the large 500-nm R_2 response in Fig. 3 was fit with a double exponential function, and this template was overlaid with the large 440-, 480-, and 520-nm ERC responses and provided a good fit. The 400- and 540-nm ERC responses were of lower SNR and were not fit well by the template. ERC data in Fig. 3 was collected with 30 nm FWHM stimuli. In the rhodopsin expression system, photon energy does not affect the kinetics of the state transitions in rhodopsin, which is consistent with the univariance principle.

Ground State Rhodopsin ERC Can Be Photoregenerated from Metarhodopsin-II

Previous studies have shown that the ground state of rhodopsin can be photoregenerated from Meta-II_{380} by near UV flashes delivered concurrent with its lifetime

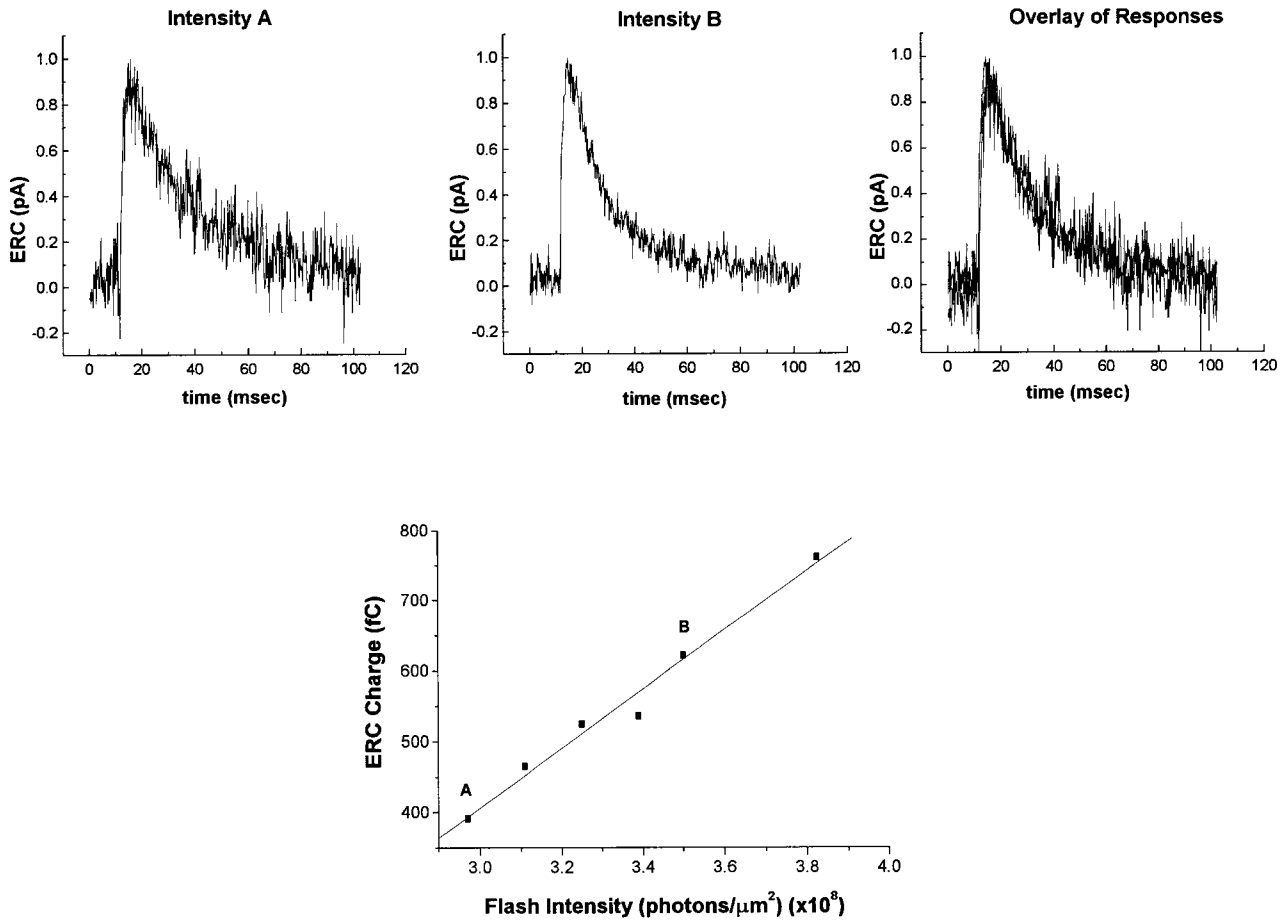

Figure 5. Tests of ERC linearity and independence. ERCs were recorded using flashes of different intensity (2.9×10^8 and 3.5×10^8 photons/μm^2) at 500 nm in a spontaneously regenerated cell held at 0 mV. Responses were normalized to the peak of R_2, and the responses were overlaid. The kinetics of R_2 relaxation appear otherwise identical regardless of flash stimulus intensity. A graph of the charge motion versus flash intensity at 500 nm is also shown and is fit by a line with slope of 420.62 fC/10^8 photons per μm^2 ($R = 0.99039$, $P < 0.000138$). The A and B marks above the line reflect the ERC responses shown.

(Williams, 1964, 1968; Williams and Breil, 1968; Cafiso and Hubbell, 1980; Drachev et al., 1981; Arnis and Hofmann, 1995). Photolysis of Meta-II generated inverted ERP signals (Cone and Cobbs, 1969; Ebrey, 1968; Cafiso and Hubbell, 1980; Drachev et al., 1981). To investigate whether photoregeneration could be assayed with ERC measurements, 500-nm flashes were used to extinguish the ERC into background cell noise, whereupon 350-nm flashes (70 nm FWHM) overlapping the Meta-II absorption (350 nm, 8.02×10^7 photons/μm^2) were delivered immediately and in rapid succession. The number of near UV flashes (1–5, 5, 10, and 20) delivered was varied to affect an increasing dose of photoregeneration stimulus to the Meta-II remaining in the cell. Immediately after the near UV flashes were delivered, additional flashes at 500 nm were used to measure the level of regeneration as the ERC R_2 charge. Under the conditions of these experiments, the expected lifetime of Meta-II at room temperature in a membrane environment is on the order of several minutes (van Breugel et al., 1979; Parkes and Liebman, 1984). Fig. 7 A shows ERC responses from an experiment where 5, 10, or 20 350-nm flashes were given to promote photoregeneration of ground state rhodopsin from Meta-II. The top trace in each case is the ERC response to the first 500-nm flash in the series used to initially extinguish the signal. The middle shows the response to the last 500-nm flash indicating the level of extinction into the whole-cell current noise. The bottom shows the first flash at 500 nm after 5 (left), 10 (middle), or 20 (right) UV flashes. As the number of UV flashes is increased, the size of the recovered 500-nm ERC signal becomes similar to that found before the UV flashes. The ERC R_2 current waveform in response to 500-nm flashes after the UV flashes is comparable in size and kinetics to the 500-nm signal that preceded bleaching whether 5, 10, or 20 UV stimuli were delivered. This data suggested that the ground state of the pigment (11*c*Ret) is regenerated during the photoconversion process. In this cell, the amount of ERC R_2

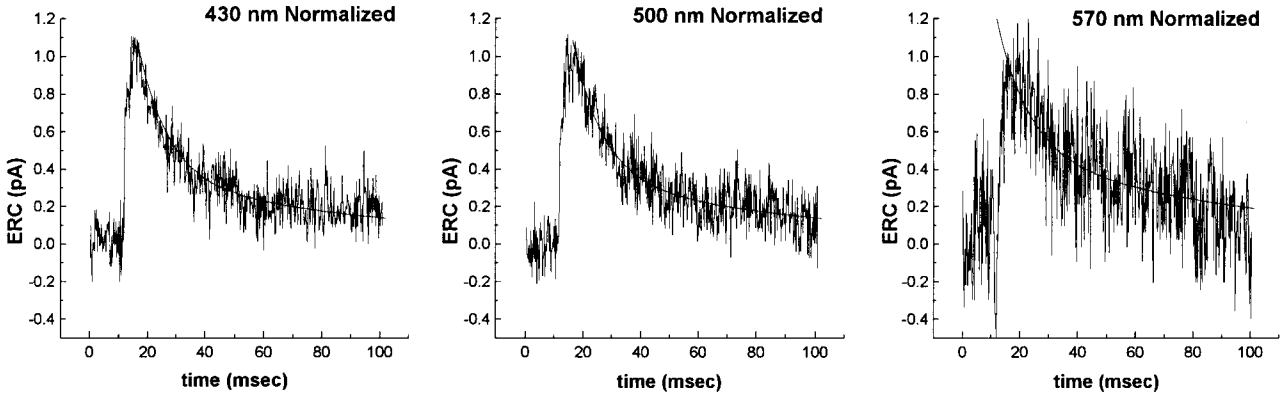

Figure 6. Test of the univariance principle. The first ERC responses to flashes at 430, 500, and 570 nm in a single fused giant cell regenerated with 11*c*Ret are shown. Responses are from a cell that had spontaneously regenerated and was held at +30 mV. Stimuli were generated with 70-nm bandpass filters and intensities were: 430 nm (3.63×10^8 photons/μm^2), 500 nm (4.08×10^8 photons/μm^2) and 570 nm (3.38×10^8 photons/μm^2). ERCs at each stimulation wavelength were smoothed by adjacent point averaging (8), and then normalized to the smoothed peak of the R_2 current such that the normalization was not to the noise band. The ERC R_2 signal resulting from the 500-nm flash was then fit with a double exponential template. This template was then overlaid with the R_2 signal from the 430- and 570-nm responses and provided a good fit at the other stimulation wavelengths (see also Fig. 3).

charge increased over the time period of successive extinctions. The underlying mechanism is not yet clear (see discussion). Fig. 7 B shows the percent of ERC charge recovered after 5 (65%), 10 (74%), or 20 (87%) UV flashes, measured against the UV flash dose. The period of time needed to deliver 5, 10, or 20 UV flashes was 27, 67, or 182 s, respectively, in this experiment. Since the kinetics of spontaneous regeneration has a time constant of ~3 min (Fig. 1 D), ERC responses after 10 or 20 UV flashes could be significantly affected by chemical regeneration with chromophore rather than photoregeneration. Therefore, the charge recovery in response to one to five UV flashes was examined (Fig. 7 B). By the third UV flash, the process of regeneration had stabilized (~55%) at the UV intensity used and no significant additional charge recovery was found when two additional UV flashes were given. The amount of charge regenerated by three to five UV flashes was similar to that which regenerated after five flashes of the same intensity in the experiment described above. Only 11 s were required to deliver the three UV flashes, making it highly unlikely that any significant chemical regeneration had contributed to the 55% charge recovery. Thus, UV stimuli promoted a large fractional recovery of R_2 charge in a time frame that is much more rapid than the kinetics of spontaneous ERC regeneration by dark adaptation. These results strongly suggest that the ERC can be photoregenerated by additional photons overlapping the Meta-II bandwidth. The quantal efficiency appears favorable to studying the mechanism in greater detail.

In most cells receiving UV stimuli, no apparent ERC charge motion occurred above the noise level of the cell. However, in a few large giant cells, apparent UV flash–induced ERC signals were identified even without any signal smoothing to suppress noise. An example is shown in Fig. 7 C, where a response to a UV (350-nm) flash is generated immediately after extinction of ERC signals with 500-nm stimuli. The UV-induced ERC signal is small and has a negative (inverted) R_2-like response. An unconstrained third order polynomial fit the UV R_2 signal and also demonstrated the inverted R_2 signals. An ERC generated with a 500-nm flash after dark adaptation in the same cell is shown to demonstrate the magnitude of the normal R_2 charge motion. The time to peak of the positive 500- and negative 350-nm–induced R_2 signals was 5.9 and 12.2 ms, respectively. The ratio of the inverted to noninverted R_2 charge was 0.175 (0.099 in another smaller cell).

9-cis-Retinal Regeneration Results in ERC Signals Consistent with Isorhodopsin

Cells were regenerated with 9*c*Ret to test the feasibility of ERC investigation of rhodopsin activation in analogue visual pigments. Analogue visual pigments are usually formed from WT opsin and a synthetic retinal known to have unique properties (e.g., to block Meta-II formation), but could also be formed from synthetic retinals and site-specific opsin mutants. The naturally occurring 9*c*Ret analogue forms isorhodopsin, a stable ground state pigment that is generated in a photostationary state with rhodopsin and bathorhodopsin (Birge et al., 1988). Once isorhodopsin is photoactivated to bathorhodopsin, the same sequence of bleaching intermediates occur as compared with normal rhodopsin activation. ERCs were recorded in three of four fused cells regenerated in 9*c*Ret and signals were uniformly small. This may in part

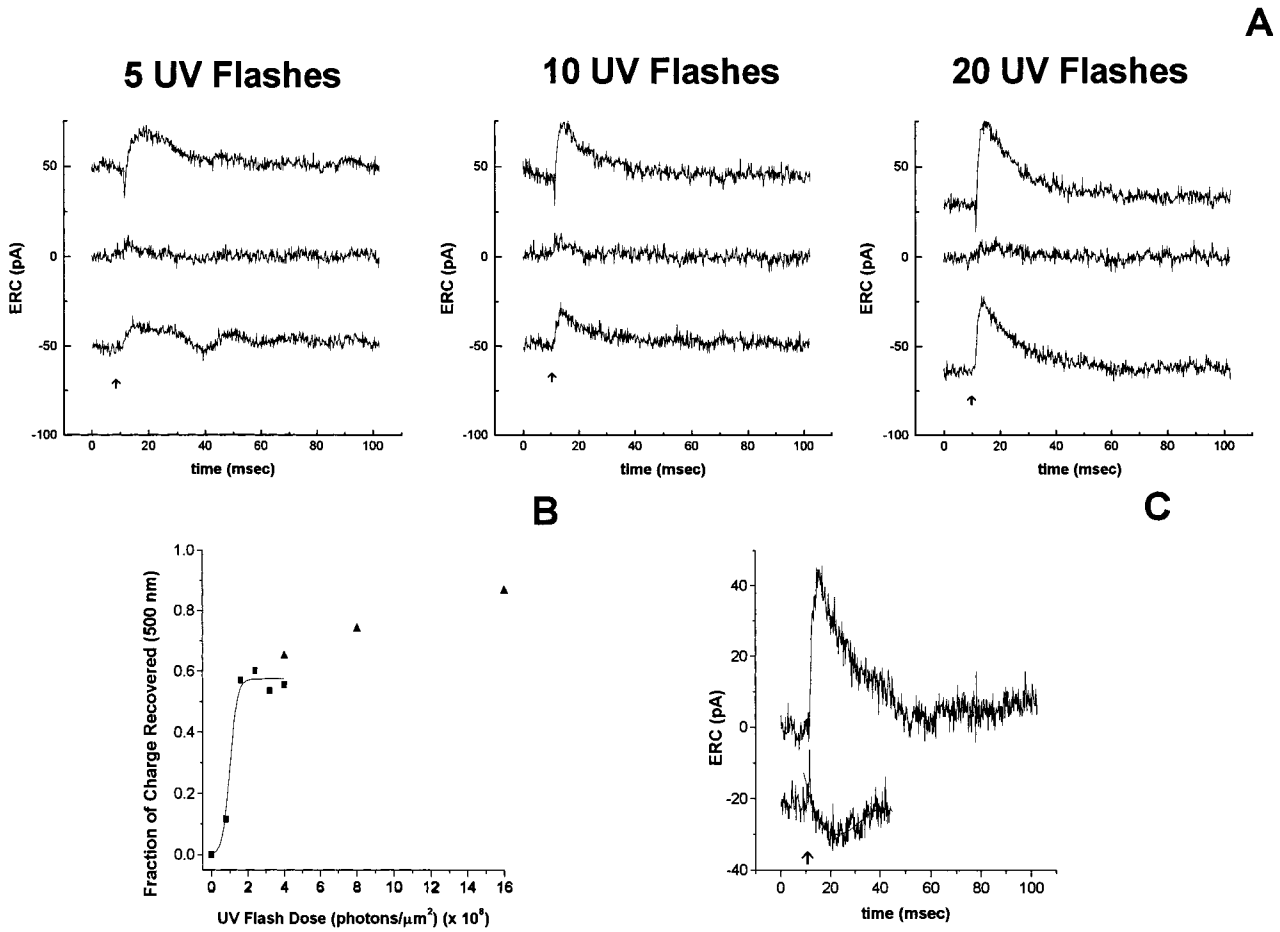

Figure 7. Photoregeneration from Meta-II$_{380}$. (A) 500-nm flashes (4.08×10^8 photons/μm^2) were used to extinguish the ERC signal into the whole-cell current noise. Immediately thereafter, near UV flashes (350 nm, 8.07×10^7 photons/μm^2) overlapping Meta-II absorption (peak 380 nm) were given. In this experiment, either 5 (left), 10 (middle), or 20 (right) UV flashes were given after the initial extinction, which required 27, 67, and 182 s, respectively, to deliver. 500-nm flashes were given immediately after the UV flashes to determine how much ground state ERC charge was recovered. In each panel, the ERC response to the first and last 500-nm flashes that initially extinguished the signal are shown (top and middle, respectively) (secondary regeneration). (Bottom) The ERC in response to first flash at 500 nm immediately after the set of UV flashes is shown. (B) The amount of recovered charge after UV flashes was normalized to the total amount of charge measured in the extinction immediately before the respective set of UV flashes to control for the increase in total R_2 charge in this cell over time. Percent regeneration is plotted versus cumulative UV flash dose for two experiments. In the first experiment, 5, 10, or 20 UV flashes were given (▲) (data shown in A). Approximately 65% of the charge was recovered after five flashes with additional charge recovered by 10 and 20 flashes. In another experiment (■), one to five UV flashes were given over 12, 7, 11, 19, and 22 s, respectively. Approximately 55% of the ERC charge was recovered by the third flash and there was little change after three subsequent flashes. These data were fit by a saturating Boltzmann function with a saturation point (A_2) of 0.575, a nodal point ($I_{1/2}$) of 10^8 photons/μm^2, and a sensitivity factor (dI) of 0.19×10^8 photons/μm^2) (below). (C) Inverted ERC signals with a slower time course compared with positive R_2 were seen in response to 350-nm flashes. ERC signals are shown for a single representative cell (61.9 μm, C_{mem} = 126.2 pF) in response to 500- and 350-nm flashes (secondary regeneration). After the 500-nm flashes had extinguished ERC R_2 signals, 350-nm flashes were given. The upper trace is the ERC response to a 500-nm flash and the lower trace is the response to a 350-nm flash on the same time scale. Without constraint, third order polynomials fit the inward going charge motion. Note an apparent reversed R_1 phase in the response of the larger cell: $Q = (A_1 - A_2)/\{1 + \exp[(I - I_{1/2})/dI]\} + A_2$ ($A_1 = 0$).

be related to the cell sizes used [C_{mem} 85.7, 11.6 (probably a single cell), and 48.6 pF]. Fig. 8 shows primary (left) and secondary (middle) extinctions of ERCs with 500-nm flashes for a fused cell regenerated with 9*c*Ret. ERC signals in fused WT-HEK293 cells regenerated with 9*c*Ret were smaller than those regenerated with 11*c*Ret in the population of cells studied. However, the ERC R_2 waveform was similar. P_t was determined by flash series extinction at 500 nm (70 nm) for this cell and found to be 1.03×10^{-9} μm^2, which is similar to the P_t we calculate for isorhodopsin at peak extinction at 483 nm (5.55×10^{-9} μm^2). This value is arrived at by first calculating the molecular cross section (α_λ) from the extinction coefficient for isorhodopsin at 483 nm (44,000 $M^{-1} \cdot cm^{-1}$)

($\alpha_\lambda = 3.82 \times 10^{-21} * \epsilon_\lambda$) ($\alpha_\lambda = 1.68 \times 10^{-8}$ μm^2) and multiplying α_λ by the quantal efficiency of isorhodopsin of 0.33 (Crouch et al., 1975). At the flash intensities used in these experiments (4.08×10^8 photons/μm^2), ~90% of isorhodopsin pigment molecules should absorb at least one photon, with ~55% of these being odd-numbered isomerizations that would proceed forward to bleaching and ~45% being even-numbered isomerizations that would result in photoconversion to ground state species. Thus, P_t could be suppressed by photoregeneration at the flash intensities used.

Kinetic Comparison of Mutant and WT Visual Pigments with the ERC

One way to exploit the sensitivity of the ERC technique is to investigate charge motions in mutant rhodopsins. We generated stable, high-level producing (~10^6 opsins/single cell), HEK293S cell lines of several human rod opsin mutants altered at single amino acids that could support proton exchange processes in the membrane region (Sullivan and Satchwell, 2000). Here we demonstrate the nature of the ERC signals obtained from D83N and E134Q opsin pigments regenerated with 11*c*Ret. Our previous work suggested that the kinetic relaxation of the R_2 phase of WT human rhodopsin in WT-HEK293S giant cells was kinetically complex (Sullivan and Shukla, 1999). In that study, we found that double exponentials were typically required to reliably fit large R_2 relaxations >100 ms after the flash. In this study, we further our kinetic analysis of WT R_2 relaxation and compare R_2 relaxations from the two mutant pigments to WT.

Fig. 9 shows ERC signals in response to the first 500-nm flash after primary regeneration and secondary recovery in fused giant cells containing WT, D83N, or E134Q human rhodopsins. The WT pigment generated strong R_1 signals during the primary bleach. R_1 signals are rarely seen during the secondary or subsequent extinctions indicating that, if present, the size is below the limits of detection at the flash intensities used. Large (>40 pA) WT ERC signals typically require two exponentials to fit the time course of the R_2 relaxation over the first 100 ms. Residuals are shown beneath the ERC waveforms. R_1 signals were not observed in D83N rhodopsin during primary extinction in cells with R_2 charges of the same order as seen in fused WT cells that had R_1 signals. Like WT, the D83N R_2 relaxation typically requires two exponentials to reliably fit its relaxation. However, D83N signals appear to lack the "stretched" exponential appearance seen in many large WT signals during the 100 ms after the flash. The E134Q ERC signal was distinctly different from the WT signal. R_1 signals were not observed during primary extinctions. Moreover, the outward R_2 signals in E134Q rhodopsin-expressing cells were markedly simplified in comparison with WT or D83N ERCs. The relaxation was brief and required only a single exponential to fit its decay. Like WT ERCs, D83N and E134Q ERC signals extinguished with successive flashes and had spectral sensitivity consistent with pigments absorbing ~500 nm (Sakmar et al., 1989; Nathans, 1990).

To begin to characterize R_2 relaxation, single or double exponential functions were fit to a large number of WT, D83N, and E134Q R_2 signals from many cells of similar size range. Time constants associated with R_2 relaxation, but not R_1, are essentially independent of C_{mem} (Sullivan and Shukla, 1999). Time constants were extracted from the first and second exponential terms (τ_a, τ_b). Since the identification of the respective components is dependent upon their weighting, it is possi-

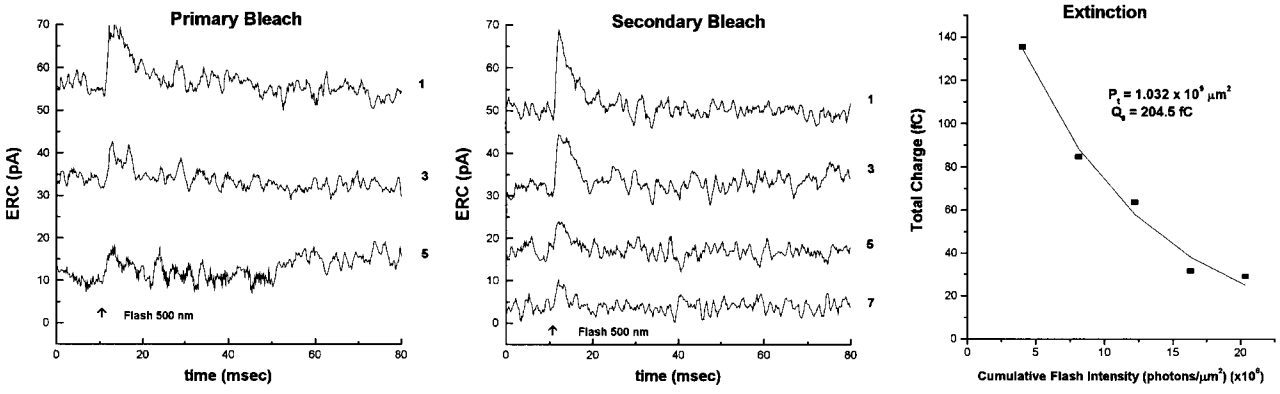

Figure 8. 9-cis-Retinal regenerates ERC signals. Cells were exposed to 25 μM 9*c*Ret complexed to 2% FAF-BSA in regeneration buffer for over 30 min. (Left) ERC signals from a cell that was photolyzed with 500-nm flashes after the primary regeneration are small and extinguish with successive flashes. (Middle) After 10 min of dark adaptation, spontaneous recovery of ERCs was found with similar R_2 kinetics compared with those found after primary extinction. Similar results were found in two additional cells. Holding potential for two cells was +30 mV and for one cell was 0 mV. (Right) An ERC charge extinction analysis allowed P_t to be extracted from the single exponential fit for the secondary regeneration. The cell was held at 0 mV. P_t was 1.03×10^{-9} μm^2.

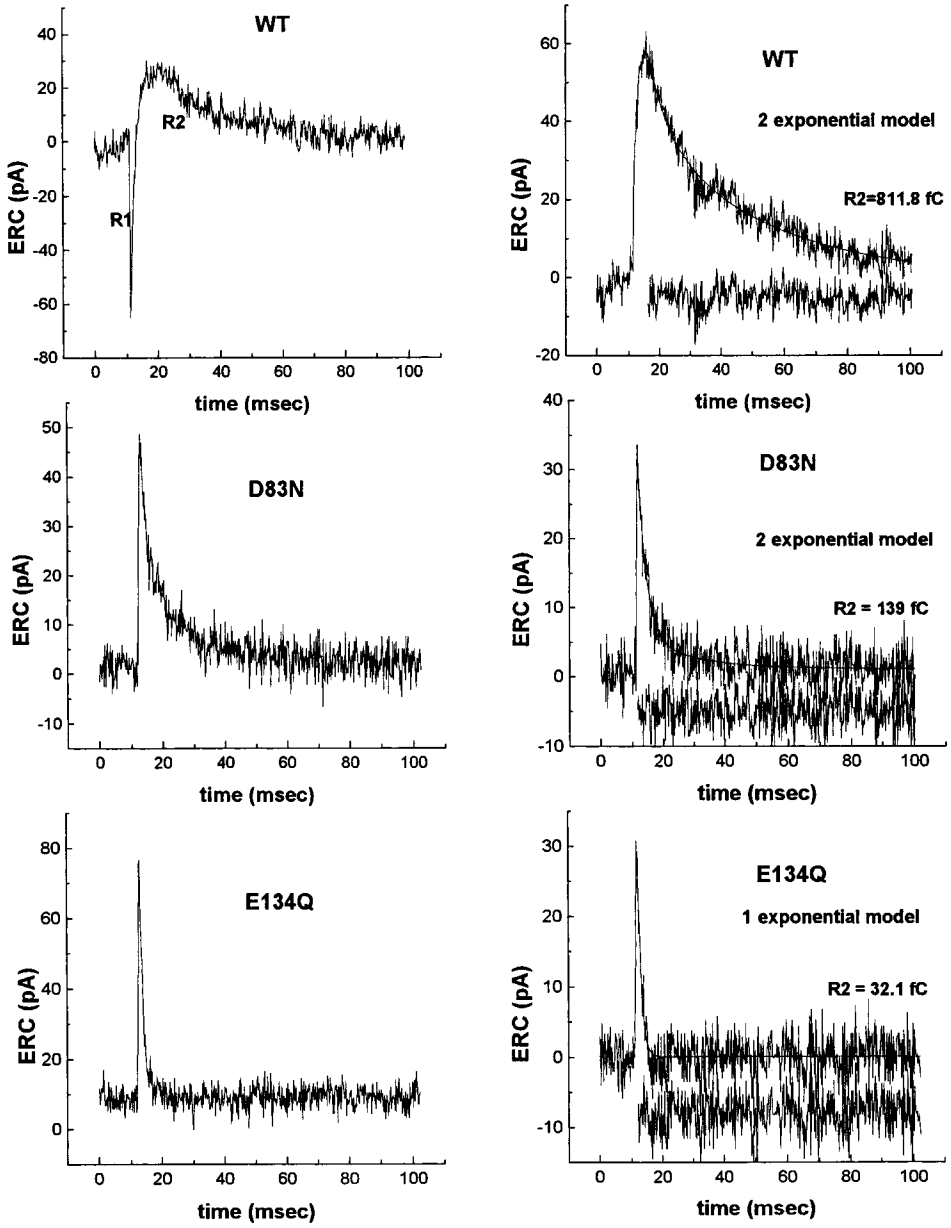

Figure 9. Comparison of ERC signals in WT, D83N, and E134Q human rhodopsins. The first ERC response to a 500-nm flash stimulus after primary regeneration (left) and after secondary recovery (right) is shown for WT human, D83N, and E134Q rod rhodopsin. In comparison with the WT pigment, D83N and E134Q lack R_1 signals on the primary extinction series. D83N has a simpler R_2 kinetic relaxation and loses the stretched exponential characteristic seen in the WT ERC, whereas the E134Q ERC is a simple outward current of short duration that is well fit by a single exponential. Attempts were made to fit single, double, or triple exponential models to secondary ERC R_2 relaxations. If each exponential corresponds to a unique rate leading from a particular electrical state (Markovian), the WT and D83N R_2 relaxations are reliably fit by the sum of two exponentials, consistent with three unique electrical states, whereas the single exponential fitting of the E134Q R_2 relaxation suggests a two-state model. Residuals are shown beneath each fitted R_2 waveform. R_2 relaxations were fit with double ($A, B > 0$) or single exponential models ($B = 0$) of the form:

$$ERC(t) = A \cdot e^{-(t-t_0)/\tau_a} + B \cdot e^{-(t-t_0)/\tau_b},$$

where τ_a and τ_b and A and B are the time constants and weights of the fitted exponentials, and t_o is the time at which fitting was initiated (just after the peak of R_2).

ble that the τ_b constant could be assigned to the τ_a data set if the weighting of the τ_a component is small or unreliable (e.g., lower SNR). Therefore, all the time constants obtained for R_2 relaxation were placed into a total ensemble, and histograms were generated from these populations for the WT, D83N, and E134Q datasets (Fig. 10, A–C). The WT pigment demonstrated a broad skewed distribution suggestive of density around three time constant ranges, whereas the E134Q distribution was simple and symmetrical and the D83N distribution was intermediate. To quantitatively characterize the ensemble of time constants, Gaussian distribution functions were fit to each histogram. The WT histogram was reliably fit by a sum of three gaussian distributions, centered at 4.1, 12.5, and 26.4 ms (Table I). There were also residuals with time constants longer than the three fitted distributions. This analysis demonstrates the kinetic complexity of the WT R_2 relaxation and supported the conclusion of a minimum of three charge states with distinct lifetimes (see discussion). The D83N histogram was reliably fit to the sum of two Gaussian functions centered at 3.7 and 10.7 ms, still leaving some residuals. These time constants are comparable with the two fastest time constants measured in the first 100 ms of WT R_2 relaxations, whereas the third τ found in WT appears to be missing (Table I). The

E134Q histogram was distinctly different from both WT and D83N, requiring only a single Gaussian function with a peak centered at 4.4 ms. This single peak overlaps with the fastest time constant seen in the WT and D83N pigments (Table I). This work establishes an initial approach to parameterize the R_2 relaxation. The intent is to use this approach as a means to quantify differences between WT and mutant ERC kinetics during the biochemically important time period of the R_2 signal.

DISCUSSION

In earlier work, we established that, after regeneration with 11*c*Ret, ERC signals could be recorded from both single and fused HEK293S cells expressing high levels of WT human opsin to their plasma membranes (Sullivan, 1998; Sullivan and Shukla, 1999). The ERC originated from plasma membrane opsin that was regenerated with chromophore and the amount of charge motion was proportional to the size of the fused giant cell, consistent with the quantity of opsin expressed in the plasma membrane. The fused cell technique offered the advantage of a larger SNR, permitting more complex experiments and observations of greater complexity in the ERC signal (e.g., the R_1 phase) when compared with the single cell system. In this early work, an action spectrum for the R_2 signal was consistent with a normal rhodopsin pigment, but the bandwidth of the filters used (70 nm) made it difficult to conclusively rule out the contribution to the ERC response of other spectral pigment states with absorption ~500 nm. Critically, it was demonstrated that the application of time-resolved ERC recording to expressed rhodopsin improved measurement sensitivity between 10^7- and 10^8-fold when compared with other contemporary methods used to study expressed visual pigments.

In the current experiments, we applied the expression ERC tool to investigate physical properties of WT rhodopsin expressed in HEK293S cells. ERC measurements are consistent with normal properties of WT human rhodopsin such as the absorbance spectrum, photosensitivity, univariance, and photoreversibility from Meta-II. The utility of the expression ERC tool was expanded on in the experiments reported here by demonstrating successful measurements of ERCs in cells regenerated with the analogue chromophore 9*c*Ret. Moreover, ERCs of two mutant pigments D83N and E134Q demonstrate qualitative and quantitative differences with respect to WT ERCs. These results strongly suggest that the expression ERC approach could be productively expanded to investigate a broad range of rhodopsin activation properties of analogue visual pigments and mutant visual pigments, thus embracing a structure–function approach applied to both the chromophore and remote environments of rhodopsin.

On Recording ERCs from Expressed and Regenerated Visual Pigments in Giant HEK293S Cells

When fused giant cells are regenerated (primary) with 11*c*Ret in the dark, ERC signals are obtained on high intensity flash stimulation (10^8 photons/μm^2) with essentially identical waveform to the ERCs of vertebrate amphibian photoreceptors (Hestrin and Korenbrot, 1990; Makino et al., 1991; Sullivan and Shukla, 1999; Sullivan et al., 2000). The total charge motion in fused giant cells typically exceeds that found in amphibian rod photoreceptors. Both the R_1 and R_2 signals of the WT ERC were observed. The R_1 signal is not well resolved kinetically and is not likely to be since R_1 is thought to report very early charge separation events in the chromophore environment that are orders of magnitude outside the bandwidth of whole-cell patch clamp recording. Thus, only the amplitude of R_1 charge could be measured, but not its rise time. The R_2 signal is completely resolved in these experiments given that the rise of R_2 to its peak is observable in most cells, as is the R_1 to R_2 transition during primary bleaching. The ERC time scale that was well resolved in these experiments extends out from ~400 μs after the flash. This is sufficient to cover the entire time course of the Meta-I to Meta-II equilibrium at room temperature. At higher bandwidth and lower temperatures, the formation of Meta-I from lumirhodopsin could probably be examined. The temporal limits of investigation of rhodopsin electrical state transitions with whole-cell recording will

TABLE I

Comparison of R_2 Relaxation Kinetics in WT, D83N, and E134Q Human Rhodopsins

Pigment	Time constants			Peak Weightings		
	τ_1	τ_2	τ_3	A_1	A_2	A_3
		ms				
WT*	4.10 ± 0.07	12.45 ± 0.6	26.44 ± 0.3	45.2 ± 4.1	52.0 ± 6.3	24.0 ± 2.8
D83N	3.67 ± 0.19	10.67 ± 1.78	—	28.8 ± 7.8	37.1 ± 10.2	—
E134Q	4.43 ± 0.52	—	—	33.9 ± 6.0	—	—

The mean (± SEM) of the time constants and their relative weightings were determined from fitting the sums of gaussian distributions to histograms of all time constants extracted from exponential fittings of the R_2 relaxation.

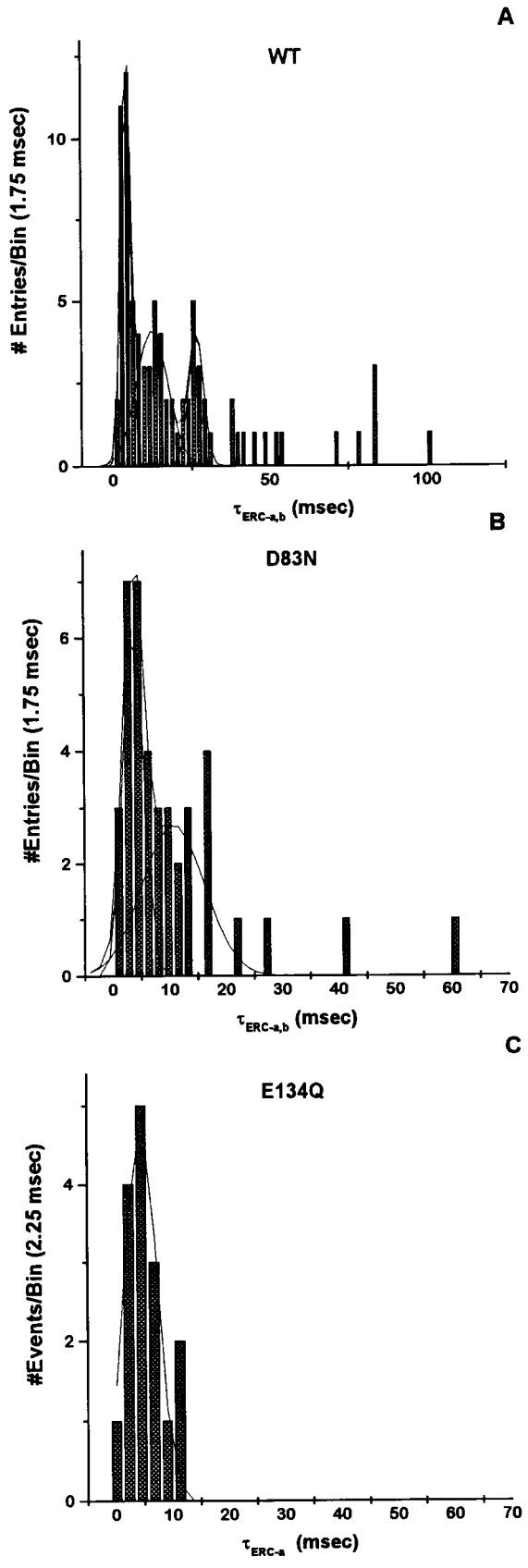

be the rise time of the flash stimulus, the speed and sensitivity of the amplifier and digitization hardware, cellular capacitance and access resistance, and the decreased SNR expected due to greater noise at wider bandwidths.

To regenerate rhodopsin from opsin apoprotein constitutively expressed in these cells, a FAF-BSA technique previously used to regenerate rhodopsin from opsin in intact rod outer segments (McDowell, 1993) was adapted to the HEK293S fused cell expression system. The regeneration kinetics (≈3 min) are similar to rates in intact photoreceptors ($\tau_{1/2} \approx 1$ min, complete by 10 min; McDowell, 1993). The combination of fusing single cells to form giant cells and the use of FAF-BSA regeneration permitted much larger ERC signals and the spontaneous recovery of the ERC signal during post-bleach dark adaptation.

Experiments reported here indicated that the source of 11*c*Ret during spontaneous dark regeneration is internal to the cell that is recorded. Several bleach and recovery cycles were required to completely exhaust the source of chromophore in the presence of extracellular NH_2OH. If regenerating 11*c*Ret chromophore originated from the outer surface of the plasma membrane or external to the cell (e.g., released by other cells on the coverslip or from recording chamber surfaces), then NH_2OH should rapidly prevent ERC recovery by converting retinaldehydes to oximes, which do not form visual pigments. The only other potential source of chromophore is internal to the cell under recording, shielded from reaction with extracellular 10 mM NH_2OH. Once NH_2OH was applied to the bath, plasma membrane visual pigment was partially bleached and spontaneously regenerated over several cycles before the source of intracellular chromophore became exhausted and ERCs did not recover. Prompt recovery followed washout of NH_2OH and perfusion of 25 μM 11*c*Ret plus FAF-BSA in recording buffer. These experiments suggest that 11*c*Ret can enter the retinal binding pocket when presented from either side of the membrane. The data also provides indirect evidence that

Figure 10. R_2 state complexity in WT, D83N, and E134Q rhodopsins. An ensemble of all time constants from exponential fitting ($\tau_{a,b}$) was used to construct histograms for WT (A), D83N (B), and E134Q (C) rhodopsin R_2 relaxations. The intracellular pH of the WT and D83N studies was 6.5, whereas in the E134Q studies it was 6.0, 6.5, 7.0, 7.5, or 8.0. Sums of Gaussian distributions functions were fitted to the histograms of time constants. WT rhodopsin requires at least three Gaussians, D83N requires two, and E134Q requires a single Gaussian to reliably represent the time constant histograms. Individual Gaussians are drawn over each peak and the composite Gaussian (sum) traces the envelope of represented density. Time constants and errors from the fitting are shown in Table I.

NH_2OH is impeded from permeating the plasma membrane of the HEK293 cells in E-1/I-1 solutions because if it had, then the spontaneous regeneration should have been promptly quenched. That ERCs are recordable when NH_2OH has access to the extracellular surface of membrane-oriented rhodopsin indicates that visual pigment regenerated in the dark is not reacting with this agent, consistent with the resistance of the ground state of rod rhodopsin to NH_2OH. NH_2OH does not affect the rate of formation of Meta-II (Johnson, 1970). Persistence of ERC R_2 signals in NH_2OH also suggests that buildup of thermal bleaching intermediates such as Meta-II, Meta-III, or M_{470} cannot be contributing to the charge motions of the ERC signals during secondary extinctions because the all-trans-retinal in the ligand pocket of these rhodopsin conformations would react rapidly with NH_2OH to form opsin and the oxime adduct and extinguish the signal entirely.

One of the major advantages of the FAF-BSA/α-d-tocopherol regeneration technique in fused giant cells is the spontaneous recovery of visual pigment and ERC signals without the need for reinstallation of 11*c*Ret into the recording chamber. A similar process has been reported for retina isolated away from pigment epithelium and apparently reflects limited photoreceptor stores of 11*c*Ret (Cone and Brown, 1969; Knowles and Dartnall, 1977). Makino et al. (1991) also found spontaneous regeneration of ERC signals and used extracellular NH_2OH (10 mM) to quench the process, indicating that a major fraction of chromophore originated from outside the cell (e.g., partitioned onto chamber surfaces) during active delivery of retinals to the recording chamber. In the experiments reported here, no 11*c*Ret or 9*c*Ret was unintentionally added to the chamber in our experiments other than perhaps a small amount on the small coverslip fragment holding the giant cells. The FAF-BSA/vitamin E technique appears to be an efficient way to load chromophore into HEK293 cells that express visual pigments. Similar success was found by McDowell (1993) for intact rod photoreceptors using FAF-BSA and for Jones et al. (1989), where interphotoreceptor retinoid-binding protein was used. The experiments reported by McDowell (1993) were conducted with a 10-fold molar excess of 11*c*Ret (25 μM) over opsin and demonstrated pseudo–first-order kinetics. Rotmans et al. (1974) demonstrated that the regeneration rate of opsin in bleached outer segment fragments ($\tau_{1/2} \approx 10$ min) was similar to the decay of Meta-II at 25°C (≈7 min half-life) and proposed that 11*c*Ret enters the ligand-binding pocket only after all-trans-retinal has vacated the environment. FAF-BSA can be viewed as a nonspecific retinoid binding protein (Noy and Xu, 1990; Livrea et al., 1991; Winston and Rando, 1998). The likely mechanism of its action is that FAF-BSA effectively solubilizes chromophore in an aqueous environment and permits efficient transfer into lipid membranes. Once partitioned into cellular membranes, retinoid transfer into bleached pigments can be rapid (Noy and Xu, 1990; McDowell, 1993; Stecher et al., 1999). Curiously, the rate limiting enzyme in the visual cycle of rodent rod photoreceptors, all-trans-retinol dehydrogenase/reductase, is also expressed in kidney (Haeseleer et al., 1998). This raises the interesting hypothesis that HEK293S cells may have some capacity for retinoid metabolism. HEK293S cells are a suspension-adapted clone of transformed human embryonic kidney cells. As such, they are likely to express both general human cell housekeeping genes as well as some genes specific for the kidney. This cellular system has been a popular expression environment for heterologous genes including human and bovine opsins over the last decade (Nathans et al., 1989; Nathans, 1990).

Spontaneous regeneration of visual pigment after 11*c*Ret loading in FAF-BSA/vitamin E provides parsimonious support of ERC experiments. The regeneration of ERCs in WT-HEK293S cells from an internal source of 11*c*Ret provides a clear advantage for complex experiments where charge motions must be compared against different conditions (e.g., action spectra determination). Two properties of ERCs measured in this environment are under further active investigation (Brueggemann and Sullivan, manuscript in preparation). First is the loss of the inward R_1 signal after post-bleach spontaneous regeneration. The time to peak of the R_2 signal is slowed approximately twofold when the R_1 signal is present (Sullivan and Shukla, 1999), possibly suggesting that the R_1 signal represents additional state transformations. In cells that were primarily loaded with 11*c*Ret and studied under whole-cell recording for periods of time >30 min, a slow accumulation of R_2 charge (approximately twofold) occurred (see Fig. 7 A). The mechanism of this process is not yet clear.

The Ground State of Rhodopsin Is the Source of the ERC Signal

Strong evidence is demonstrated that ERC signals result from activation of the ground state of human rhodopsin in the plasma membrane of fused giant cells and that no other additional spectral states are contributing to these measurements. Evidence supports the conclusion that the identity of the chromophore regenerating visual pigment is 11*c*Ret, which forms a PSB^+-H with K296 of the opsin apoprotein. The action spectrum of the ERC of WT human rhodopsin, when stimulated through 30-nm bandpass filters, was well fit by a scaled normalized template of the absorbance spectrum of WT human rhodopsin purified from the same cell line used for ERC studies. The action spectrum was obtained from cells that had already had their ERCs ex-

tinguished and had undergone spontaneous recovery. These experiments allow the conclusion that the ground state of rhodopsin is the one that regenerates upon dark adaptation after primary ERC extinction. Thus, during dark adaptation, the Meta-II state must decay with hydrolysis of the Schiff base to form opsin, which then can subsequently react with 11*c*Ret to form a protonated Schiff base at K296. From our previous work on spectral sensitivity, which was conducted with 70-nm bandpass filters, the action spectra was much broader than rhodopsin absorbance. Data from the experiments reported here shows that this outcome was the result of stimulus bandwidth, and not the presence of additional spectral states that were contributing to charge motion. Specifically, there were three pigments that could have contributed to "recovery" of the ERC when later stimulated with 500-nm stimuli: Meta-III$_{465}$ and Meta$_{470}$, both resulting from thermal Meta-II$_{380}$ decay (Hofmann et al., 1992), and isorhodopsin resulting from photoregeneration from early intermediates. The formation and lifetime of Meta-III and Meta$_{470}$ are consistent with the kinetics found for ERC recovery (≈3.0 min). However, if these states contributed substantially to the ERC, the action spectrum would not have been fit by the absorbance of rhodopsin and the signals should have been promptly extinguished by 10 mM NH_2OH (Hofmann et al., 1992; Lewis et al., 1997). Given the difference in peak absorbance of bovine and human rhodopsin, these three pigments in isolation would have produced action spectra with peaks around 460, 475, and 483 nm. The human rhodopsin absorbance spectrum, peaking at 493 nm, provided a good fit to the action spectra peak and there was no evidence of a significant blue shift of the ERC data. In addition, the bandwidth of the ERC action spectrum was consistent with rhodopsin absorbance. Thus, we conclude that the pigment underlying the ERC after primary regeneration and secondary recovery is rod rhodopsin, which was not sensitive to NH_2OH in the dark. The rapid recovery of ERC signal over 10-min periods suggests that long-lived photointermediates such as Meta-III or Meta$_{470}$ are not extensively populated in this expression system. If these or other pigment states are present, their contribution to the ERC must be minimal. This conclusion is substantiated by the similar P_t values for ERC extinction after primary regeneration and secondary recovery. If additional states were involved it is likely that the P_t parameter would have changed significantly.

R_2 Extinction Photosensitivity Is Consistent with Rhodopsin Activation

The ERC signal can be extinguished with successive flashes in a fashion similar to rhodopsin bleaching in photoreceptors and with similar photosensitivity. The mean and maximum P_t values (2.6×10^{-9} and 5.0×10^{-9} μm^2, respectively) determined from exponential extinction decays are consistent with a rhodopsin photopigment but are lower than expected (1.0×10^{-8} μm^2), taking the product of the molecular cross section of human rhodopsin at 493 nm ($\alpha_{493} = 1.528 \times 10^{-8}$ μm^2, see materials and methods) and the known quantal efficiency ($\gamma = 0.67$) (Dartnall, 1968). The mechanism for the approximately twofold suppression of P_t is considered. One would not expect any significant pigment orientational effect in the fused cell system because rhodopsin is expressed in a membrane with an essentially spherical geometry at the time of recordings and any orientation should increase P_t. The P_t values obtained from ERC extinctions of R_2 in amphibian rods ($7.6 \pm 2.2 \times 10^{-9}$ μm^2) originate predominantly from an A_2 pigment with a lower peak extinction coefficient than human rhodopsin (≈30,000 vs. 40,000 $M^{-1} \cdot cm^{-1}$) (Makino et al., 1991). Since cells were regenerated with 11*c*Ret, an A_1 pigment is expected and found upon purification of rhodopsin from the same cell line. Therefore, the suppressed values of P_t must have a different origin. Our findings may reflect, in part, the variability of extracting the P_t parameter from extinction experiments (Makino et al., 1991). The accumulation of bleaching intermediates is unlikely because the extinction coefficients of Meta-III or Meta$_{470}$ are similar to that for rhodopsin and would not be expected to suppress P_t. Moreover, the accumulation of these intermediates was essentially excluded by ERC persistence in NH_2OH (and further P_t suppression) and the fitting of the ERC action spectrum by the absorbance spectrum of WT rhodopsin.

Photoregeneration from early intermediate states with high quantal efficiency for photoconversion (e.g., bathorhodopsin, lumirhodopsin) can definitively lower P_t estimates for the absorbing pigment (Williams, 1964, 1965). Makino et al. (1991) found no photoregeneration in ERC experiments on rod and cone photoreceptors when P_t was measured using flash strengths that were typically about an order of magnitude less intense than used here but with durations ~20-fold longer (300 μs) that probably overlapped with the Meta-I lifetime and the Meta-I ⇔ Meta-II equilibrium. Flashes of this duration were, however, unlikely to overlap significantly with the lifetimes of earlier intermediates that have higher quantal efficiency of photoconversion (Williams, 1964, 1965, 1974). At room temperature in these experiments, the only bleaching intermediates that could overlap with the 14-μs flash duration are bathorhodopsin, the blue-shifted intermediate, and lumirhodopsin. Lumirhodopsin is completely formed by 1 μs at room temperature (Lewis et al., 1989), and is likely to have been the most populated state during the

flashes presented. The flash duration in these experiments would not overlap the rate of Meta-I formation at room temperature (100 μs) (Sengbusch and Stieve, 1971). The stimuli used in these experiments should have no influence on the Meta-I ⇔ Meta-II equilibrium, which correlates in part with the R_2 time course (Ebrey, 1968; Spalink and Stieve, 1980). In extracting P_t from R_2 extinction, we are assessing early photochemical processes of absorption through examination of charge motions of later conformational states that are thermal and not photochemical in origin. If we use the mean P_t obtained at 500 nm (2.6×10^{-9} μm^2), we can calculate the quantal efficiency assuming realistically that the molecular cross section is constant (1.23×10^{-8} μm^2). This results in an estimate for γ of 0.21 that is only ~32% of the known value of 0.67 determined from small bleaches.

How could γ be decreased to explain the suppression of P_t? In fact, Williams (1964, 1965, 1966, 1974) have shown that γ is a function of light intensity. When the flash intensity is infinitely strong, γ should approach zero. γ is expected to decrease in proportion to the intensity of the flash stimulation because photoconversion becomes increasingly likely (even-numbered absorptions) from intermediates with lifetimes of the same order as the flash duration. Hagins (1955) and Williams (1964, 1965, 1974) have shown that the maximum fraction of rhodopsin bleached in a single brief flash can be only 50% because of this process. At the flash intensities used in these experiments (e.g., 500 and 70 nm FWHM, 4.08×10^8 photons/μm^2), we estimate the fraction of rhodopsin molecules absorbing at least one photon to be ~0.963 using the crude estimates obtained from the Poisson distribution (see materials and methods). However, only odd-numbered absorptions go on to bleaching, whereas even numbered absorptions photoconvert. The fraction of even-numbered photoregenerating absorptions is ~50% at the flash intensity used. Therefore a maximum of 50% of rhodopsin molecules bleach with each flash, although there are sufficient photons in a single flash to bleach all molecules present. The amount of rhodopsin bleaching with each flash, then, is a constant fraction of unbleached molecules remaining. This explains why the extinction followed a single exponential decay function. It also explains why P_t is suppressed by at least 50% in our measurements. The R_2 signal reports only those rhodopsin molecules that absorb an odd number of photons and move forward through later intermediates to bleaching. It is important to mention that the ERC R_2 kinetics should not be influenced at all by photoregeneration because the flash duration is about two orders of magnitude more brief than the electrical state transitions measured. The shape of the R_2 waveform does not change with sequential flashes even though the amplitude decreases and no evidence for photoregeneration was found when examining the extinction of the R_2 signal or the homogeneous kinetics of R_2 relaxation with different flash intensities. Thus, our findings are consistent with a significant suppression of P_t of WT rhodopsin, likely because of the high probability of early state photoconversion using the stimuli employed in these experiments. The intermediate likely to be significantly populated during the highest photon fluxes in these experiments is lumirhodopsin since it is completely formed by 1 μs and is the only state present during the bulk of photon irradiance (rise time ≈ 5 μs). High intensities were used to obtain good estimates of the cross section (α) in the spectral measurements and were maintained throughout because of the high SNR obtained in ERC recordings. In fact, P_t approximates the value expected when stimulus intensities (500 nm) are nearly a log-fold lower (see results). In future experiments, the effects of a range of flash intensities on P_t and quantal efficiency will be investigated. In addition, we will also investigate the mechanism for the marked suppressive effect (≈1 log) of NH_2OH on P_t, which appears to be a novel finding. We speculate that NH_2OH has the capacity to bind in retinal binding pocket and perhaps alter the local chromophore environment in the ground state in such a manner as to result in altered photochemical properties.

Photoregeneration of Meta-II Can Be Detected with ERC Measurements

Experiments were conducted to test whether the ERC can be used to study rhodopsin photoregeneration from the Meta-II state. These experiments were motivated by earlier studies that reported reversed ERP signals from the Meta-II state upon near UV stimulation (Cone and Cobbs, 1969; Ebrey, 1968; Drachev et al., 1981; Cafiso and Hubbell, 1980). As discussed above, photoregeneration from early intermediates is likely to be responsible for the suppressive effect on estimation of P_t using the ERC method. To further explore photoregeneration as a molecular conformational process, we tested whether the ground state of rhodopsin could be achieved by photolytic activation of Meta-II, which has a lifetime accessible to xenon flash stimulation and cellular ERC measurement. Near UV flashes overlapping with Meta-II_{380} absorption and lifetime were presented immediately after extinction of 500 nm ERC responses and promoted rapid recovery of the ERC signal in a manner inconsistent with the normal chemical regeneration by 11*c*Ret. Meta-II is known to have an extinction coefficient slightly larger than rhodopsin, and photocoversion of Meta-II to rhodopsin has been reported to occur with a quantal efficiency of ~0.2 (Williams, 1968; Williams and Breil, 1968). Using estimates

of the extinction coefficient for Meta-II between 33,000 and 49,200 $M^{-1}\,cm^{-1}$ and the Poisson equation, the fraction of Meta-II molecules absorbing at least one photon would be 25–35%/flash with 80–90% of these being single photon absorptions at the 350-nm photon densities delivered (8.02×10^7 photons/μm^2). The inverted ERC signals that were only seen in large cells are consistent with inverted ERP signals that have been recorded from the retina (Arden et al., 1966; Cone, 1967; Ebrey, 1968; Cone and Cobbs, 1969). These results are consistent with a net reversal of charge flow during photoregeneration from Meta-II. The reverse state path is likely to be different compared with the forward activation pathway given that the amount of charge is much smaller (10–20%) and appears to have a considerably slower time course with respect to the peak times of the positive R_2 signals that associate with Meta- II formation. Complete reversibility of the transitions would be expected to result in charge motions of the same magnitude but different polarity. Arnis and Hofmann (1995) recently showed that photoregeneration of rhodopsin from the active Meta-II state proceeds by isomerization of the chromophore and Schiff base reprotonation, but the ground state was achieved on a much slower time scale and was due to thermal and not photochemical conformational changes. Such slow events would not be seen in these current recordings, but might be reflected in ERP (voltage) recordings where the charge flow can be integrated on the membrane capacitance. Therefore, the small inverted ERC signals that we see with UV flashes could reflect dipolar rearrangements in the chromophore pocket or the reprotonation of the Schiff base, perhaps from the E113 protonated counterion, which is located more toward the extracellular surface of rhodopsin (Baldwin, 1993; Jager et al., 1994). Or it could reflect release of protons from the cytoplasmic surface (Ostroy, 1974). Future experiments will focus on the rate of thermal disappearance of the Meta-II state from which photoregeneration most likely occurs and the molecular origin of the inverted charge flow (e.g., pH dependence). The quantal efficiency of the photoregeneration process appears favorable to study the mechanism in greater detail in even larger cells.

9-cis-Retinal Regenerates ERCs from WT Opsin

When WT-HEK293S cells are regenerated with 9*c*Ret, ERC signals are recordable upon 500-nm flash photolysis. 9*c*-Ret regenerates a visual pigment, presumed to be isorhodopsin (peak $\approx$ 483 nm), which would broadly overlap with the 70-nm band stimulus. That ERC signals can be recorded from a "natural" analogue pigment provides evidence to support a role for the ERC in investigation of a wide variety of analogue visual pigments that are known to have unique properties. For example, certain locked analogues are known to prevent energy uptake by preventing isomerization (Bhattacharya et al., 1992). Others block the bleaching sequence at discrete spectral states, for example, 9-cis-desmethylretinal blocks the thermal bleaching pathway at Meta-I (Ganter et al., 1989). Investigation of analogue pigments can now be extended to the vectorial charge flows that are orthogonal to the chromophore plane. Similarly, analogue retinals could regenerate opsins with engineered side-chain mutations in the ligand-binding pocket to investigate environmental interactions that shape chromophoric properties and activation behavior.

Kinetic Analysis of R_2 ERC Signals of WT and Mutant (D83N and E134Q) Pigments

A major challenge in structure–function studies of visual pigments has been the preparation of sufficient mutant protein in expression systems for biophysical or biochemical analysis. The ERC method improves detection sensitivity by 10^7–10^8-fold, allowing measurements of conformational activation in an ensemble of regenerated rhodopsin molecules in the physiologically intact environment of a single fused giant cell (Sullivan and Shukla, 1999). In applying the ERC to mechanistic studies of conformational activation, a number of rhodopsin mutants were screened at sites of potential proton exchange reactions in the membrane environment of the protein. The time course of the expression ERC R_2 signal overlaps with the temporal scale of Schiff base deprotonation and Meta-II formation, as well as the related proton uptake into the cytoplasmic face of the pigment and the conformational transition to the biochemically active Meta-II_b state (Arnis and Hofmann, 1993). Since known mutants can affect various steps in this activation process, a quantitative structure–function investigation on opsin mutants was initiated in this ERC study. A mutation in the PSB^+-H environment (D83N) on the second α helix was found to perturb the kinetics of the R_2 ERC phase. A mutation on the cytoplasmic face of the third α helix (E134Q), at a residue known to be a gatekeeper to both proton uptake and the related generation of the transducin docking environment, results in loss of most of the ERC R_2 signal except for the fast initial process.

The R_2 signal is well resolved in cellular ERC measurements and overlaps temporally with critical events leading to biochemical activation of rhodopsin. WT rhodopsin R_2 relaxation kinetics are an easily accessible aspect of the total ERC signal and are invariant to intensity or wavelength of stimulation as found in these experiments. Therefore, the R_2 relaxation should be a reliable parameter to evaluate for understanding conformational dynamics. A quantitative analysis of R_2 re-

laxation in WT rhodopsin should serve not only to begin characterization of the state complexity of charge motion on the millisecond time scale, but also serve for comparison of mutant pigments that might be affected in some aspect of R_2 electrical state transitions. WT rhodopsin R_2 relaxation was first characterized by fitting sums of exponentials to a set of WT ERC waveforms and generating an ensemble of time constants ($\tau_{a,b}$). We assumed that the ensemble of time constants would represent the kinetic aspects of the signal even with any slight heterogeneity (e.g., due to cell size) that might affect only the fastest aspects of the relaxation (Sullivan and Shukla, 1999). Treating the entire time constant data set as an ensemble is reasonable because the assignment of a value to τ_a or τ_b is somewhat arbitrary given that the short time constant may not have been weighted or fit in a particular ERC signal and a longer time constant was then assigned to τ_a. In fact, there is some overlap in the assignments (Sullivan and Shukla, 1999). Also, analysis of an ensemble of ERC signals is more likely to identify additional complexity for quantification than can be obtained in fittings to single ERC waveforms. A histogram was generated from the ensemble of the total WT time constants data set (Fig. 10 A). The histogram is not consistent with a single distribution of time constants. While there was a prominent peak around 4 ms, there is significant weighting outside this band leading to a skewed distribution with additional peaks being apparent. To characterize the distribution of time constants in the R_2 relaxation, we fit sums of Gaussians to the (skewed) histogram of the entire $\tau_{a,b}$ ensemble. We attempted fits of one, two, three, and four Gaussians to the data. With this data set, a reliable fit of the sum of three Gaussians was obtained that was independent of bin width. Three Gaussian peaks were centered around 4.1, 12.45, and 26.4 ms, and the errors in the fitting results are shown in Table I. The natural conclusion from this analysis is that there are a minimum of three distinct electrically active states in the WT R_2 relaxation at room temperature in WT rhodopsin. We speculate that the underlying molecular basis of the three fitted time constants are likely to represent processes related to Schiff base deprotonation, proton uptake, and α helical movements associated with conformational activation. However, other interpretations are possible. For example, the capacitative, or AC-coupled nature of the ERC could reflect forward and reverse movements of charges (e.g., protons, sidechains), in particular molecular environments, leading to a series of coordinated charge separation and recombination events, each satisfying a zero-time integral expected for pure capacitative components (e.g., see Hong et al., 1992). We have not demonstrated a net DC component to the ERC. Further investigation will be necessary to examine these hypotheses and to determine the uniqueness of the time constants determined. We anticipate that dissection of the ERC R_2 signal can be achieved with mutations at protein side chains likely to participate in charge transfer events.

ERC signals from D83N rhodopsin (regenerated with 11*c*Ret) appear slightly simplified in comparison with WT. The R_2 signal appears WT in nature, but shorter in comparison to the broad stretched relaxation of the WT pigment. D83N ERCs were subjected to R_2 relaxation time constant analysis, and the sum of two Gaussian distributions was required to best fit the total time constant histogram. Peaks were identified at 3.67 and 10.67 ms, and the errors in the fitting are shown in Table I. These times appear comparable to the fast and medium time constants in the WT pigment that was measured under identical conditions. The third and longest time constant of the R_2 relaxation in WT (26.4 ms) is missing in the D83N pigment. We suspect this is likely to represent a distinct property of the D83N pigment since R_2 relaxation in D83N ERCs have a different waveform compared with WT. In summary, D83N loses the R_1 signal during primary bleaches and its R_2 relaxation loses the "stretched exponential" characteristic of the WT R_2 relaxation.

The D83N mutation is known to slightly blue-shift the absorbance of rhodopsin, which is consistent with an alteration of the Schiff base environment in the ground state pigment, resulting from the isomorphic loss of the protonated carboxyl group of aspartate (Fahmy et al., 1993; Rath et al., 1993). However, D83N pigment in detergent has the capacity to form Meta-II and to activate transducin, but these properties have not been examined under rapid time-resolved conditions (Sakmar et al., 1989; Zhukovsky and Oprian, 1989; Nathans, 1990; Cohen et al., 1993). Weitz and Nathans (1993) concluded that the D83N mutation leads to a more favored formation of Meta-II compared with WT rhodopsin by analysis of difference spectra. The D83 sidechain is located in the immediate environment of the protonated Schiff base and is a highly conserved residue in G-protein–coupled receptors (Baldwin, 1993). Therefore, it could play an as yet unrealized role in rapid activation processes. Fahmy et al. (1993) found a shift in carboxyl signals in the WT Meta-II/rhodopsin infrared difference spectra that was lost in the D83N mutant. They suggested that the D83 sidechain undergoes an increase in hydrogen bonding during Meta-II formation, although they could not explicitly rule out a transient deprotonation/reprotonation reaction on the path to Meta-II. Ganter et al. (1988, 1989) suggested that the formation of Meta-I from lumirhodopsin was associated with carboxyl groups in the membrane environment undergoing such reactions. This is an area where ERC recordings are likely to be useful because of the extended band-

width and profound relative sensitivity compared with most spectroscopic techniques. The apparent loss of the R_1 signal is particularly interesting because this signal is believed to originate from charge separation of the protonated Schiff base from its counterion during isomerization (Trissl, 1982; Birge, 1990a,b). It may also be that later thermal transitions contribute to the inward R_1 charge flow and that the D83N mutation may prevent these states during primary extinction, where we usually see R_1 signals. Since the recording conditions are otherwise constant between WT-, D83N-, and E134Q-expressing cells (e.g., similar access resistance and similar ranges of membrane capacitance), it is unlikely that the loss of the R_1 signal is purely due to changes in the measurement under whole-cell voltage clamp (Okajima and Hong, 1986). The loss of R_1 signal in the D83N pigment leads us to consider that sidechain interactions in the ligand binding pocket near the Schiff base could contribute to R_1. The loss of R_1 in the WT pigment after primary extinction may simply mean that the spatial order of such interactions is not rapidly achieved under the conditions of these experiments. Finally, the apparent simplification of the R_2 relaxation in D83N may indicate that the path to Meta-II is slightly different with respect to the WT pigment, even though Meta-II ultimately results. Further experiments will be necessary to investigate these ideas as we use a variety of approaches to dissect the R_2 relaxation into quantifiable biophysical processes.

ERC signals from E134Q rhodopsin have little complexity in comparison with WT and demonstrate no R_1 and a brief R_2 relaxation always well fit by a single exponential. When R_2 relaxation time constant analysis was applied to the E134Q pigment, a single Gaussian was needed to fit the time-constant histogram. The value of the peak was 4.4 ms, which was comparable within error to WT fast phase. The timing of the fast phase did not appear to change when the cytoplasmic pH was held at different constant values over the range from 6.0 to 8.0. The E134 sidechain is known to be essential to proton uptake into the cytoplasmic face of rhodopsin during normal Meta-II formation given that the E134Q mutant binds zero protons in comparison with the two adsorbed by the WT pigment (Arnis et al., 1994; Parkes and Liebman, 1984). The sites of binding of the protons are unknown, but the E134 sidechain could titrate one proton. The loss of the medium and slow ERC time constants and the stretch beyond 50 ms in the WT R_2 relaxation suggest that these components might represent proton movements or other charge motions gated by proton uptake. E134Q, when regenerated with 11*c*Ret in the dark, is capable of activating transducin in an enhanced manner in comparison with the WT pigment after light stimulation (Franke et al., 1992; Cohen et al., 1993). The E134/R135 charge pair is known to be an essential switch to transducin docking and activation and is screened from solution once transducin is bound to R* (Franke et al., 1992; Ernst et al., 1995; Fahmy and Sakmar, 1993; Acharya and Karnik, 1996). During photoactivation to R*, a rigid body motion of α helix VI relative to α helix III (the location of E134/R135) has been detected. This results in helix VI being displaced outward from the disk membrane into the cytoplasm, although the magnitude of the vectorial movements are not yet clear (Farrens et al., 1996; Altenbach et al., 1996; Han et al., 1996). The E134Q mutation promotes movements of the III and VII α helices in the dark that are not affected by light and do not affect the subsequent movement of α helix VI. What results is a partial activation of the receptor in the darkness or constitutive activity (Kim et al., 1997). The movements of α helices may be normally coupled, but can still occur independently in the presence of environmental perturbation (e.g., mutation). Since spectral Meta-II formation is not perturbed in E134Q, we suggest that the residual fast ERC signal in this mutant represents the charge motion associated with Schiff base deprotonation. In preliminary experiments, the residual R_2 time constant of E134Q did not demonstrate sensitivity to intracellular pH over the range of 6.0 to 8.0 and might reflect the pH-insensitive component of the ERP related to Schiff base deprotonation (Bennett et al., 1980; Lindau and Ruppel, 1985; Arnis and Hofmann, 1993). By elimination, the remaining medium and slow time constants of the WT R_2 relaxation could be associated with proton uptake into the cytoplasmic face and the subsequent conformational transformation of the rhodopsin that is gated by this chemical potential (e.g., macrodipole movements of α helices). If so, then these later time constants in the WT pigment should be responsive to changes in intracellular pH or to molecular conditions that prevent the conformational activation of the molecule that allows transducin binding. Further experiments will be necessary to decipher the molecular origin of the charge motions during R_2 and how local environment affects these transitions.

We were surprised that no R_1 signals were found in fused E134Q giant cells given that the E134 sidechain resides at the cytoplasmic face of the third α helix remote from the Schiff base environment where R_1 is thought to originate. However, total charge motion in E134Q cells is smaller than in WT cells and the R_1 signal may simply have been lost in noise, as we found for R_1 in single unfused cells expressing WT pigment regenerated with 11*c*Ret (Sullivan and Shukla, 1999). However, in a separate cell line of E134Q (E134Q-12) that expresses three to four times more mutant opsin (Sullivan and Satchwell, 2000), the R_1 signal was also missing and the R_2 relaxation is still simple and single

exponential in character (Brueggemann and Sullivan, manuscript in preparation). In future efforts, the stoichiometry of charge motion in the E134Q pigment will be compared with WT. Given that R_1 is likely to be definitively lacking, a model should be considered wherein the membrane-buried Schiff base environment near the middle of the membrane and the proton uptake environment on the cytoplasmic face of the membrane might communicate on a very rapid time scale during activation.

Although we do not yet have a molecular understanding of the simplification of the ERC R_2 signal in D83N or E134Q, such mutant pigments with uniquely different ERC signals constitute a substrate to understand the components of the normal ERC signal in WT rhodopsin. At this point, our efforts have clearly established the feasibility of using the ERC to study time-resolved and electrically active conformational changes during rhodopsin activation in WT and two mutant pigments. Future studies will focus on the molecular mechanism of R* formation and the forces that govern the molecular volume increase of the pigment during the Meta-II_a to Meta-II_b transition in WT and mutant pigments (Arnis and Hofmann, 1993).

Summary and Conclusions

The sensitivity of the expression ERC method is greatly improved when compared with other contemporary time-resolved techniques applied to rhodopsin activation and allows measurement of rhodopsin activation in single cells containing about a picogram of visual pigment. The sensitivity of this approach is dependent upon the use of gigaohm-seal, whole-cell patch clamping techniques that are capable of resolving small currents with fast time resolution. The ERC is a conformation-dependent charge motion of the same family as ionic channel gating currents. Gating current analysis of expressed mutant ionic channels has significantly extended knowledge of molecular processes of conformational activation of ionic channels, and for this reason we are applying the same approach to visual pigments that are known to be electrically active proteins. In this work, we apply the expression ERC approach to measure properties of WT rhodopsin and found that the ERC signal results from activation of the ground state of rhodopsin, given the action spectra and bleaching photosensitivity. ERC kinetics are independent of wavelength, as expected for the univariance principle, and rhodopsin can be photoregenerated from the Meta-II state. The major impact of this study resides in our success at recording ERCs from an analogue visual pigment (isorhodopsin) and from two mutant human opsins regenerated with 11*c*Ret. This study establishes the feasibility of an ERC structure/function investigation applied to the ligand binding pocket, as probed by artificial chromophores or site-specific mutations, or remote regions of the pigment, as probed by engineered mutations or chemically reactive ligands. The ERP has been similarly used in expressed mutant bacteriorhodopsin pigments to understand proton exchange mechanisms (e.g., Moltke et al., 1992; Misra, 1998). The similarity of the visual rhodopsin ERC/ERP and the bacteriorhodopsin ERP is striking and suggests that similar underlying mechanisms of conformational transitions may be conserved over evolutionary time. The ERC measures a vector of activation across the membrane plane in a population of oriented molecules under physiologically intact conditions not dissimilar to the environment of activation in a photoreceptor. We anticipate that this approach will lead to further understanding of the energies, forces, and molecular processes of rhodopsin activation on a rapid time scale.

The authors thank Drs. Michael Sheets and J. Hugh McDowell for sharing their methods on recording ionic channel gating currents from fused transfected HEK293 cells and on FAF-BSA rhodopsin regeneration, respectively. The authors acknowledge the technical assistance of Michael F. Satchwell with cell cultures. The authors appreciate the critical review of the manuscript by Drs. Bob Birge, Ken Foster, and Barry Knox before its submission and the comments of the reviewers before publication.

This work was funded by an R29 award (EY11384) from the National Eye Institute to J.M. Sullivan. Also supported, in part, by start-up funds from the Department of Ophthalmology at SUNY (which is a recipient of a Research to Prevent Blindness Award).

Submitted: 11 November 1999 Revised: 2 August 1999 Accepted: 9 August 1999 Released online: 11 October 1999

REFERENCES

Acharya, S., and S.S. Karnik. 1996. Modulation of GDP release from transducin by the conserved Glu^{134}–Arg^{135} sequence in rhodopsin. *J. Biol. Chem.* 271:25406–25411.

Altenbach, C., K. Yang, D.L. Farrens, Z.T. Farahbakhsh, H.G. Khorana, and W.L. Hubbell. 1996. Structural features and light-dependent changes in the cytoplasmic interhelical E-F loop region of rhodopsin: a site-directed spin-labeling study. *Biochemistry.* 35:13470–13478.

Arden, G.B., H. Ikeda, and I.M. Siegel. 1966. New components of the mammalian receptor potential and their relation to visual photochemistry. *Vision Res.* 6:373–384.

Arnis, S., and K.P. Hofmann. 1993. Two different forms of metarhodopsin II: Schiff base deprotonation precedes proton uptake and signaling state. *Proc. Natl. Acad. Sci. USA.* 90:7849–7853.

Arnis, S., and K.P. Hofmann. 1995. Photoregeneration of bovine rhodopsin from its signaling state. *Biochemistry.* 34:9333–9340.

Arnis, S., K. Fahmy, K.P. Hofmann, and T.P. Sakmar. 1994. A conserved carboxylic acid group mediates light-dependent proton uptake and signaling by rhodopsin. *J. Biol. Chem.* 269:23879–23881.

Baldwin, J.M. 1993. The probable arrangement of the helices in G protein–coupled receptors. *EMBO (Eur. Mol. Biol. Organ.) J.* 12: 1693–1703.

Bennett, N., M. Michel-Villaz, and Y. Dupont. 1980. Cyanine dye measurement of a light-induced transient membrane potential associated with the Metarhodopsin II intermediate in rod-outer-segment membranes. *Eur. J. Biochem.* 111:105–109.

Bezanilla, F., and E. Stefani. 1994. Voltage-dependent gating of ionic channels. *Annu. Rev. Biophys. Biomol. Struct.* 23:819–846.

Bhattacharya, S., K.D. Ridge, B.E. Knox, and H.G. Khorana. 1992. Light-stable rhodopsin. I. A rhodopsin analog reconstituted with a nonisomerizable 11-*cis* retinal derivative. *J. Biol. Chem.* 267: 6763–6769.

Birge, R.R., C.M. Einterz, H.M. Knapp, and L.P. Murray. 1988. The nature of the primary photochemical events in rhodopsin and isorhodopsin. *Biophys. J.* 53:367–385.

Birge, R.R. 1990a. Nature of the primary photochemical events in rhodopsin and bacteriorhodopsin. *Biochim. Biophys. Acta.* 1016: 293–327.

Birge, R.R. 1990b. Photophysics and molecular electronic applications of the rhodopsins. *Annu. Rev. Phys. Chem.* 41:683–733.

van Bruegel, P.J.G.M., P.H.M. Bovee-Geurts, S.L. Bonting, and F.J.M. Daemen. 1979. Biochemical aspects of the visual process XL. Spectral and chemical aspects of metarhodopsin III in photoreceptor membrane suspensions. *Biochim. Biophys. Acta.* 557: 188–198.

Cafiso, D.S., and W.L. Hubbell. 1980. Light-induced interfacial potentials in photoreceptor membranes. *Biophys. J.* 30:243–264.

Chen, C., and H. Okayama. 1988. Calcium phosphate-mediated gene transfer: a highly efficient transfection system for stably transforming cells with plasmid DNA. *Biotechniques.* 6:632–637.

Cohen, G.B., T. Yang, P.R. Robinson, and D.D. Oprian. 1993. Constitutive activation of opsin: influence of charge at position 134 and size at position 296. *Biochemistry.* 32:6111–6115.

Cone, R.A. 1967. Early receptor potential: photoreversible charge displacement in rhodopsin. *Science.* 155:1128–1131.

Cone, R.A., and P.K. Brown. 1967. Dependence of the early receptor potential on the orientation of rhodopsin. *Science.* 156:536.

Cone, R.A., and P.K. Brown. 1969. Spontaneous regeneration of rhodopsin in the isolated rat retina. *Nature.* 221:818–820.

Cone, R.A., and W.H. Cobbs. 1969. Rhodopsin cycle in the living eye of the rat. *Nature.* 221:820–822.

Cone, R.A., and W.L. Pak. 1971. The early receptor potential. *In* Handbook of Sensory Physiology: Principles of Receptor Physiology. Volume 1. W.R. Lowenstein, editor. Springer Verlag, Berlin. 345–365.

Crouch, R., V. Purvin, K. Nakanishi, and T. Ebrey. 1975. Isorhodopsin II: artificial photosensitive pigment formed from 9,13-*Dicis* retinal. *Proc. Natl. Acad. Sci. USA.* 72:1538–1542.

Dartnall, H.J.A. 1968. The photosensitivities of visual pigments in the presence of hydroxylamine. *Vision Res.* 8:339–358.

Dilley, R.A., and D.G. McConnell. 1970. Alpha-tocopherol in the retinal outer segment of bovine eyes. *J. Membr. Biol.* 2:317–323.

Drachev, L.A., G.R. Kalamkarov, A.D. Kaulen, M.A. Ostrovsky, and V.P. Skulachev. 1981. Fast stages of photoelectric processes in biological membranes. II. Visual rhodopsin. *Eur. J. Biochem.* 117:471–481.

Ebrey, T.G. 1968. The thermal decay of the intermediates of rhodopsin *in situ*. *Vision Res.* 8:965–982.

Ernst, O.P., K.P. Hofmann, and T.P. Sakmar. 1995. Characterization of rhodopsin mutants that bind transducin but fail to induce GTP nucleotide uptake. *J. Biol. Chem.* 270:10580–10586.

Fahmy, K., F. Jager, M. Beck, T.A. Zvyaga, T.P. Sakmar, and F. Siebert. 1993. Protonation states of membrane-embedded carboxylic acid groups in rhodopsin and metarhodopsin II: a Fourier-transform infrared spectroscopy study of site-directed mutants. *Proc. Natl. Acad. Sci. USA.* 90:10206–10210.

Fahmy, K., and T.P. Sakmar. 1993. Regulation of the rhodopsin–transducin interaction by a highly conserved carboxylic acid group. *Biochemistry.* 32:7229–7236.

Fahmy, K., F. Siebert, and T.P. Sakmar. 1995. Photoactivated state of rhodopsin and how it can form. *Biophys. Chem.* 56:171–181.

Farahbakhsh, Z.T., K. Hideg, and W.L. Hubbell. 1993. Photoactivated conformational changes in rhodopsin: a time-resolved spin label study. *Nature.* 262:1416–1419.

Farahbakhsh, Z.T., K.D. Ridge, H.G. Khorana, and W.L. Hubbell. 1995. Mapping light-dependent structural changes in the cytoplasmic loop connecting helices C and D in rhodopsin: a site-directed spin labeling study. *Biochemistry.* 34:8812–8819.

Farrens, D.L., C. Altenbach, K. Yang, W.L. Hubbell, and H.G. Khorana. 1996. Requirement of rigid-body motion of transmembrane helices for light activation of rhodopsin. *Science.* 274:768–770.

Franke, R.R., T.P. Sakmar, R.M. Graham, and H.G. Khorana. 1992. Structure and function in rhodopsin. Studies of the interaction between the rhodopsin cytoplasmic domain and transducin. *J. Biol. Chem.* 267:14767–14774.

Ganter, U.M., W. Gartner, and F. Siebert. 1988. Rhodopsin-lumirhodopsin phototransition of bovine rhodopsin investigated by Fourier transform infrared difference spectroscopy. *Biochemistry.* 27:7480–7488.

Ganter, U.M., E.D. Schmid, D. Perez-Sala, R.R. Rando, and F. Siebert. 1989. Removal of the 9-methyl group of retinal inhibits signal transduction in the visual process. A Fourier transform infrared and biochemical investigation. *Biochemistry.* 28:5954–5962.

Govardovskii, V.I. 1979. Mechanism of the generation of the early receptor potential and an electrical model of the rod of the intact rat retina. *Biophysics.* 23:520–526.

Haeseleer, F., J. Huang, L. Lebioda, J.C. Saari, and K. Palczewski. 1998. Molecular characterization of a novel short-chain dehydrogenase / reductase that reduces all-*trans*-retinal. *J. Biol. Chem.* 273: 21790–21799.

Hagins, W.A. 1955. The quantum efficiency of bleaching of rhodopsin *in situ*. *J. Physiol.* 129:22P.

Han, M., S.W. Lin, M. Minkova, S.O. Smith, and T.P. Sakmar. 1996. Functional interaction of transmembrane helices 3 and 6 in rhodopsin. *J. Biol Chem.* 271:32337–32342.

Hestrin, S., and J.I. Korenbrot. 1990. Activation kinetics of retinal cones and rods: response to intense flashes of light. *J. Neurosci.* 10:1967–1973.

Hodgkin, A.L., and P.M. O'Bryan. 1977. Internal recording of the early receptor potential in turtle cones. *J. Physiol.* 267:737–766.

Hofmann, K.P., A. Pulvermuller, J. Buczylko, P. Van Hooser, and K. Palczewski. 1992. The role of arrestin and retinoids in the regeneration pathway of rhodopsin. *J. Biol. Chem.* 267:15701–15706.

Hong, F.T., F.H. Hong, R.B. Needleman, B. Ni, and M. Chang. 1992. Modifying the photoelectric behavior or bacteriorhodopsin by site-directed mutagenesis: electrochemical and genetic engineering approaches to molecular events. *In* Molecular Electronics—Science and Technology. A. Aviram, editor. American Institute of Physics, AIP Conference Proceedings 262, New York, NY. 204–217.

Honig, B.H., W.L. Hubbell, and R.F. Flewelling. 1986. Electrostatic interactions in membranes and proteins. *Annu. Rev. Biophys. Chem.* 15:163–193.

Jager, F., K. Fahmy, T.P. Sakmar, and F. Siebert. 1994. Identification of glutamic acid 113 as the Schiff base proton acceptor in the

metarhodopsin II photointermediate of rhodopsin. *Biochemistry.* 33:10878–10882.

Johnson, R.H. 1970. Absence of effect of hydroxylamine upon production rates of some rhodopsin photo intermediates. *Vision Res.* 10:897–900.

Jones, G.J., R.K. Crouch, B. Wiggert, M.C. Cornwall, and G.J. Chader. 1989. Retinoid requirements for recovery of sensitivity after visual pigment bleaching in isolated photoreceptors. *Proc. Natl. Acad. Sci. USA.* 86:9606–9610.

Kersting, U., H. Joha, W. Steigner, B. Gassner, G. Gstaunthaler, W. Pfaller, and H. Oberleithner. 1989. Fusion of cultured dog kidney (MDCK) cells: I. technique, fate of plasma membranes and of cell nuclei. *J. Membr. Biol.* 111:37–48.

Khorana, G. 1992. Rhodopsin, photoreceptor of the rod cell. An emerging pattern for structure and function. *J. Biol. Chem.* 267:1–4.

Kim, J.-M., C. Altenbach, R.L. Thurmond, H.G. Khorana, and W.L. Hubbell. 1997. Structure and function in rhodopsin: rhodopsin mutants with a neutral amino acid at E134 have a partially activated conformation in the dark state. *Proc. Natl. Acad. Sci. USA.* 94:14273–14278.

Knowles, A., and H.J.A. Dartnall. 1977. The photobiology of vision. *In* The Eye. H. Davson, editor. Academic Press, Inc., New York, NY. 247–497.

Lamola, A.A., T. Yamane, and A. Zipp. 1974. Effect of detergents and high pressure upon the metarhodopsin I ⇔ metarhodopsin II equilibrium. *Biochemistry.* 13:738–745.

Lewis, J.W., C.M. Einterz, S.J. Hug, and D.S. Kliger. 1989. Transition dipole orientations in the early photolysis intermediates of rhodopsin. *Biophys. J.* 56:1101–1111.

Lewis, J.W., F.J.G.M. van Kuijk, J.A. Carruthers, and D.S. Kliger. 1997. Metarhodopsin III formation and decay kinetics: comparison of bovine and human rhodopsin. *Vision Res.* 37:1–8.

Lindau, M., and H. Ruppel. 1985. On the nature of the fast light-induced charge displacement in vertebrate photoreceptors. *Photobiochem. Photobiophys.* 9:43–56.

Livrea, M.A., L. Tesoriere, and A. Bongiorno. 1991. All-*trans* to 11-*cis* retinol isomerization in nuclear membrane fraction from bovine retinal pigment epithelium. *Exp. Eye Res.* 52:451–459.

Longstaff, C., R. Calhoon, and R.R. Rando. 1986. Deprotonation of the Schiff base of rhodopsin is obligatory in the activation of the G protein. *Proc. Natl. Acad. Sci. USA.* 83:4209–4213.

Makino, C.L., W.R. Taylor, and D.A. Baylor. 1991. Rapid charge movements and photosensitivity of visual pigments in salamander rods and cones. *J. Physiol.* 442:761–780.

McDowell, J.H. 1993. Preparing rod outer segment membranes, regenerating rhodopsin, and determining rhodopsin concentration. *Methods Neurosci.* 15:123–130.

Misra, S. 1998. Contribution of proton release to the B2 photocurrent of bacteriorhodopsin. *Biophys. J.* 75:382–388.

Moltke, S., M.P. Heyn, M.P. Krebs, R. Mollaaghababa, and H.G. Khorana. 1992. Low pH photovoltage kinetics of bacteriorhodopsin with replacements of Asp-96, -85, -212 and Arg-82. *In* Structures and Functions of Retinal Proteins. J.L. Rigaud, editor. Colloque INSERM, John Libbey Eurotext Ltd. Paris, France. 221: 201–204.

Nathans, J., C.J. Weitz, N. Agarwal, I. Nir, and D.S. Papermaster. 1989. Production of bovine rhodopsin by mammalian cell lines expressing cloned cDNA: spectrophotometry and subcellular localization. *Vision Res.* 29:907–914.

Nathans, J. 1990. Determinants of visual pigment absorbance: role of charged amino acids in the putative transmembrane segments. *Biochemistry.* 29:937–942.

Noy, N., and Z.-J. Xu. 1990. Thermodynamic parameters of the binding of retinol to binding proteins and to membranes. *Biochemistry.* 29:3888–3892.

Okajima, T.L, and F.T. Hong. 1986. Kinetic analysis of displacement photocurrents elicited in two types of bacteriorhodopsin model membranes. *Biophys. J.* 50:901–912.

Ostroy, S.E. 1974. Hydrogen ion changes of rhodopsin. pK changes and the thermal decay of metarhodopsin II_{380}. *Arch. Biochem. Biophys.* 164:275–284.

Parkes, J.H., and P.A. Liebman. 1984. Temperature and pH dependence of the metarhodopsin I–metarhodopsin II kinetics and equilibria in bovine rod disk membrane suspensions. *Biochemistry.* 23:5054–5061.

Rath, P., L.L.J. DeCaluwe, P.H.M. Bovee-Geurts, W.J. DeGrip, and K.J. Rothschild. 1993. Fourier transform infrared difference spectroscopy of rhodopsin mutants: light activation of rhodopsin causes hydrogen-bonding change in residue aspartic acid-83 during Meta II formation. *Biochemistry.* 32:10277–10282.

Reeves, P.J., R.L. Thurmond, and H.G. Khorana. 1996. Structure and function in rhodopsin: high level expression of a synthetic bovine opsin gene and its mutants in stable mammalian cell lines. *Proc. Natl. Acad. Sci. USA.* 93:11487–11492.

Rotmans, J.P., F.J.M Daemen, and S.L. Bonting. 1974. Biochemical aspects of the visual process. XXVI. Binding site and migration of retinaldehyde during rhodopsin photolysis. *Biochim. Biophys. Acta.* 357:151–158.

Sakmar, T.P., R.R. Franke, and H.G. Khorana. 1989. Glutamic acid 113 serves as the retinylidene Schiff base counterion in bovine rhodopsin. *Proc. Natl. Acad. Sci. USA.* 86:8309–8313.

Schneider, E.E., C.F. Goodeve, and R.J. Lythgoe. 1939. The spectral variation of the photosensitivity of visual purple. *Proc. R. Soc. Lond. A.* 170:102–112.

Schoenlein, R.W., L.A. Peteanu, R.A. Mathies, and C.V. Shank. 1991. The first step in vision: femtosecond isomerization of rhodopsin. *Science.* 254:412–415.

Sengbusch, G.V., and H. Stieve. 1971. Flash photolysis of rhodopsin. I. Measurements on bovine rod outer segments. *Z. Naturforschung.* 26B:488–489.

Sheets, M.F., J.W. Kyle, S. Krueger, and D.A. Hanck. 1996. Optimization of a mammalian expression system for the measurement of sodium channel gating currents. *Am. J. Physiol.* 271:C1001–C1006.

Shieh, T., M. Han, T.P. Sakmar, and S.O. Smith. 1997. The steric trigger in rhodopsin activation. *J. Mol. Biol.* 269:373–384.

Shukla, P., and J.M. Sullivan. 1998. Rhodopsin early receptor currents from fused giant cells expressing opsin. *Invest. Ophthal. Vis. Sci.* 39:974a. (Abstr.)

Spalink, J.D., and H. Stieve. 1980. Direct correlation between the R2 component of the early receptor potential and the formation of metarhodopsin II in the excised bovine retina. *Biophys. Struct. Mech.* 6:171–174.

Stecher, H., M.H. Gelb, J.C. Saari, and K. Palczewski. 1999. Preferential release of 11-*cis*-retinol from retinal pigment epithelial cells in the presence of cellular retinaldehyde-binding protein. *J. Biol. Chem.* 274:8577–8585.

Sullivan, J.M. 1996. Rhodopsin early receptor currents following flash photolysis of single cells expressing human rhodopsin. *Invest. Ophthal. Vis. Sci.* 37:811a. (Abstr.)

Sullivan, J.M. 1998. Low-cost monochromatic microsecond flash microbeam apparatus for single-cell photolysis of rhodopsin or other photolabile pigments. *Rev. Sci. Instrum.* 69:527–539.

Sullivan, J.M., L. Brueggemann, and P. Shukla. 2000. An electrical approach to study rhodopsin activation in single cells with the early receptor current assay. *Methods Enzymol.* In press.

Sullivan, J.M., and M.F. Satchwell. 2000. Development of stable cell lines expressing high levels of point mutants of human opsin for biochemical and biophysical studies. *Methods Enzymol.* In press.

Sullivan, J.M., and P. Shukla. 1999. Time-resolved rhodopsin activa-

tion currents in a unicellular expression system. *Biophys. J.* In press.
Szuts, E.Z., and F.I. Harosi. 1991. Solubility of retinoids in water. *Arch. Biochem. Biophys.* 287:297–304.
Trissl, H.W. 1982. On the rise time of the R1-component of the "early receptor potential": evidence for a fast light-induced charge separation in rhodopsin. *Biophys. Struct. Mech.* 8:213–230.
Wald, G., and P.K. Brown. 1958. Human rhodopsin. *Science.* 127: 222–226.
Weitz, C.J., and J. Nathans. 1993. Rhodopsin activation: effects on the metarhodopsin I–metarhodopsin II equilibrium of neutralization or introduction of charged amino acids within putative transmembrane segments. *Biochemistry.* 32:14176–14182.
Williams, T.P. 1964. Photoreversal of rhodopsin bleaching. *J. Gen. Physiol.* 47:679–689.
Williams, T.P. 1965. Rhodopsin bleaching: relative effectiveness of high and low intensity flashes. *Vision Res.* 5:633–638.
Williams, T.P. 1966. Limitations on the use of the concept of quantum efficiency in rhodopsin bleaching. *Nature.* 209:1350–1351.
Williams, T.P. 1968. Photolysis of metarhodopsin II. Rates of production of P470 and rhodopsin. *Vision Res.* 8:1457–1466.
Williams, T.P. 1974. Upper limits to the bleaching of rhodopsin by high intensity flashes. *Vision Res.* 14:603–607.
Williams, T.P., and S.J. Breil. 1968. Kinetic measurements on rhodopsin solutions during intense flashes. *Vision Res.* 8:777–786.
Winston, A., and R.R. Rando. 1998. Regulation of isomerohydrolase activity in the visual cycle. *Biochemistry.* 37:2044–2050.
Zhukovsky, E.A., and D.D. Oprian. 1989. Effect of carboxylic acid side chains on the absorption maximum of visual pigments. *Science.* 246:928–930.